News on QCD Physics study with the CMS detector

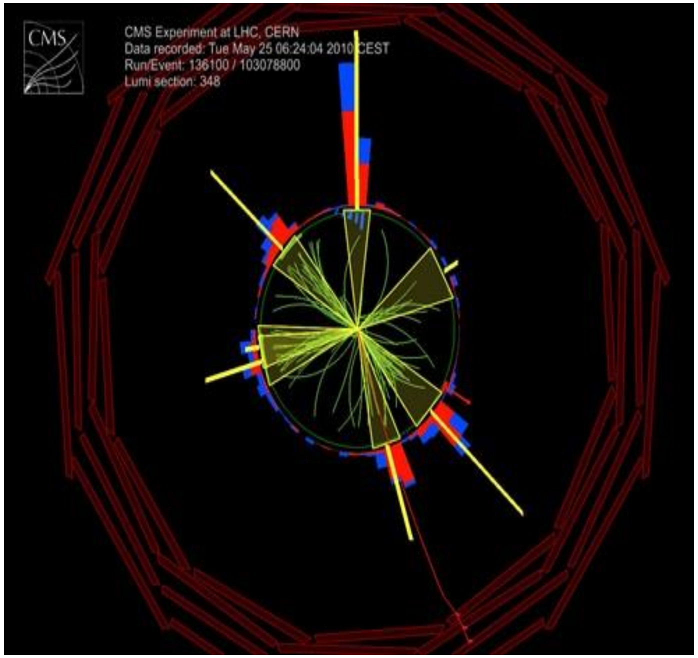

Olga Kodolova, JINR (on behalf of the CMS collaboration)

22nd Lomonosov Conference, MSU, August 21-27, 2025

Outline

- **Motivation**
- **Soft physics**
- **Hard physics**
- **Summary**

Motivation

QCD is the theory that explains strong interactions as part of the Standard Model

What is new at LHC:

Probing the new territory (x,Q^2) range

Why we need to study:

- Although QCD is the basic theory of strong interactions its parameters are still not well known.

- Important background for new territory in physics searches enormous cross section: QCD can hide many possible signals of new physics

- QCD defines the hadronization process of partons whatever interaction mediator is in the hard production vertex

What we study:

- **proton structure,**
- **constrain the strong coupling**
- **pQCD theory components**
- **study non-perturbative effects**
- **tune Monte-Carlo generators**

How do we proceed?

Practically,
we collect puzzles!

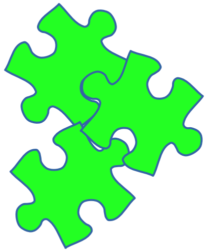

Some definitions

μ_F – factorization scale separates long and short distance physics
$\alpha_S(\mu_R)$ – running coupling constant
μ_R – renormalization scale
$Q^2 = -q^2$ – transferred momentum

Soft underlying event

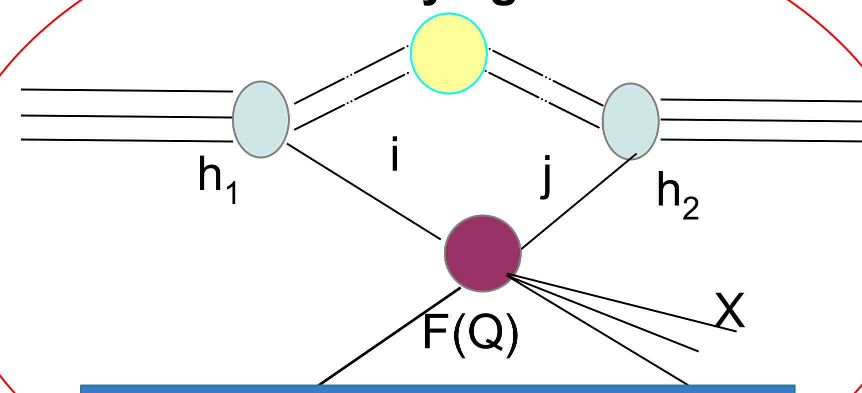

$p_1 = x_1 P_1$

$p_2 = x_2 P_2$

Hard interaction: production of the high-p_T objects

Factorization property

$$\sigma(P_{h_1}, P_{h_2}) = \sum_{i,j} \int dx_1 dx_2 f_{i/h_1}(x_1, \mu_F^2) f_{j/h_2}(x_2, \mu_F^2) \hat{\sigma}_{ij}(p_1, p_2, \alpha_S(\mu_R), Q^2; \mu_F^2, \mu_R^2)$$

Parton distribution function (PDF)

Partonic cross-section computed in pQCD

$$\hat{\sigma}_{ij} = \alpha_S^k \sum_n \left(\frac{\alpha_S}{\pi}\right)^n \sigma_{ij}^n$$

Soft interaction: production of the low-p_T hadrons

Fixed order pQCD

How do we proceed

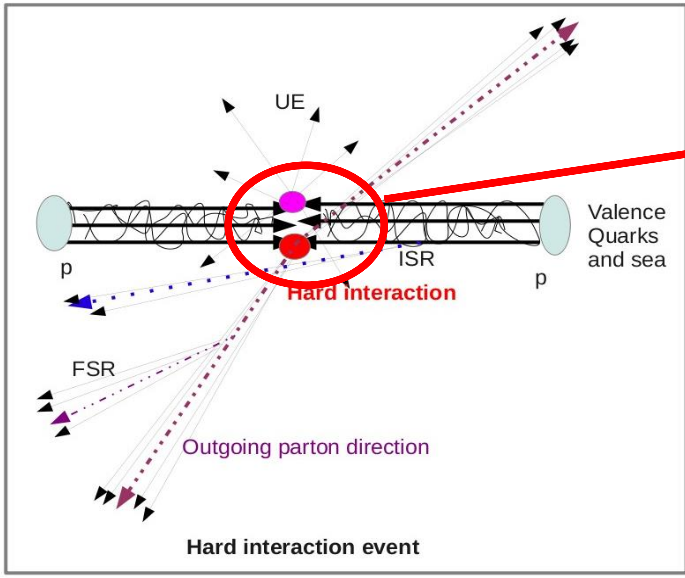

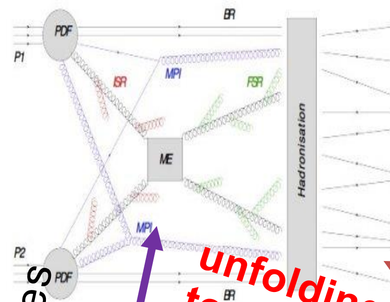

particles

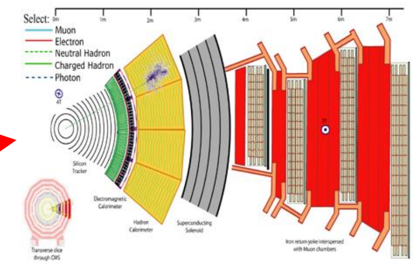

propagation towards particles level

unfolding towards particles level

ill-posed problem

Reconstructed particles, reconstructed jets
Measured Cross-sections
Multiplicity
Rapidity
Momentum of Particles and Jets, missing E_T

Hard interaction cross-section
Parton Distribution Functions
Parton showering details

Theory blocks:
- Perturbative QCD (pQCD):
LO, NLO, NNLO calculations: ME + parton showering (PS), threshold resummation
- non-pQCD: (Multi-parton interactions (MPI), String/Cluster fragmentation models)

Soft particle production

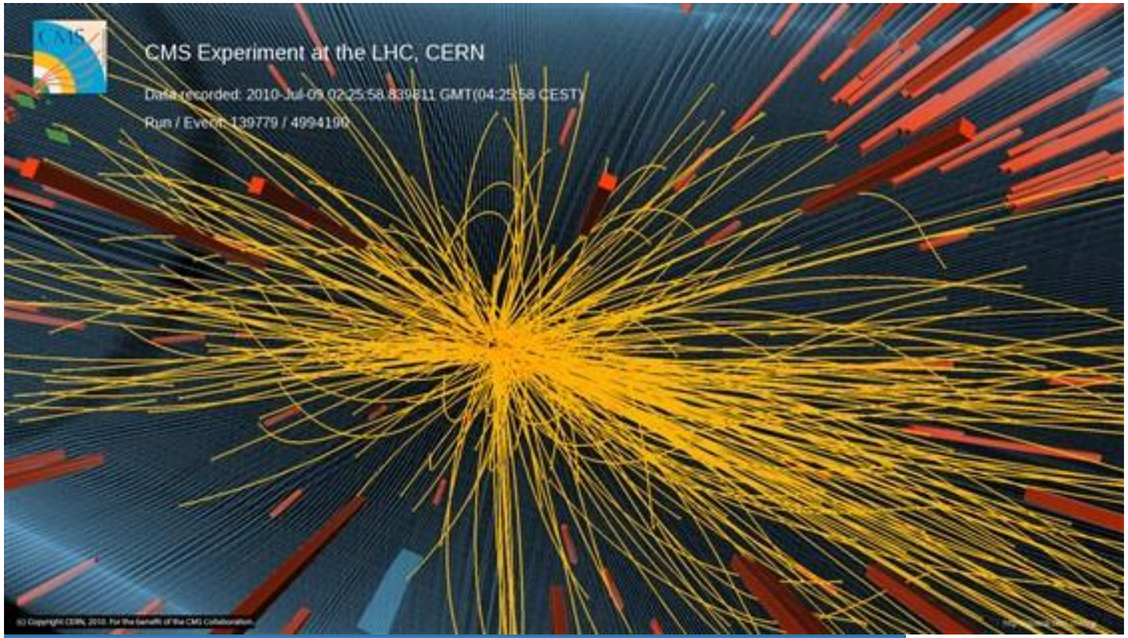

Charged particle multiplicity
Scaling, correlations
Underlying event

p_T & x_T & limiting fragmentation

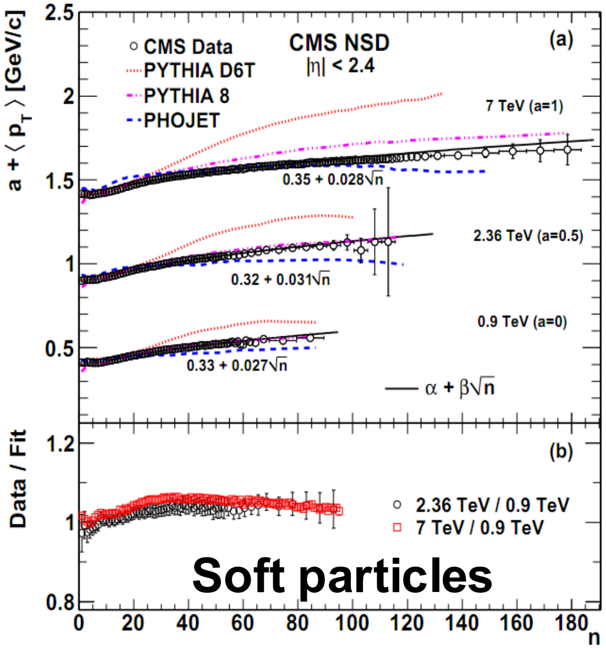

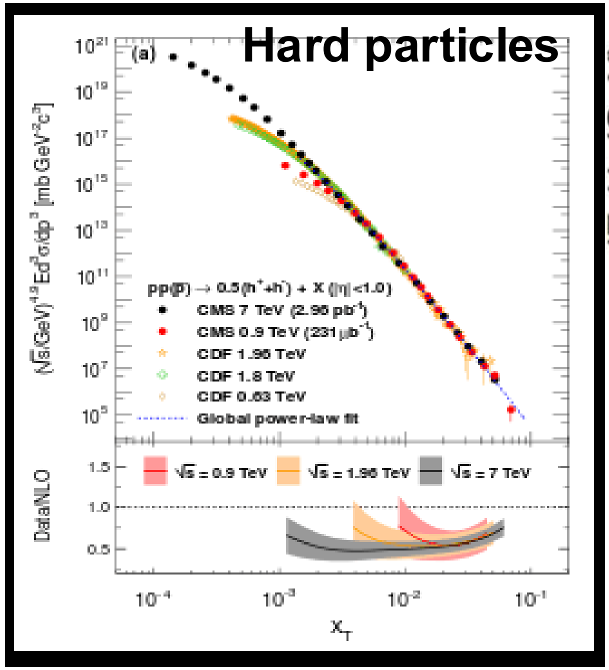

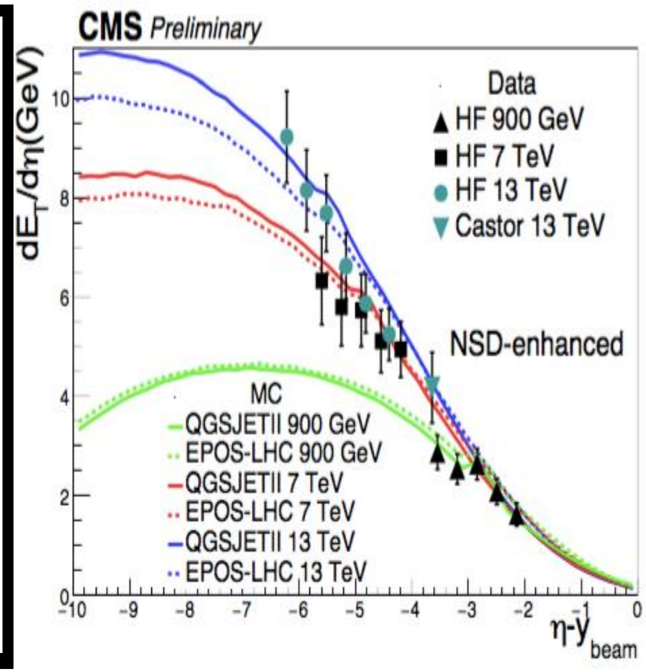

The rise of the $\langle p_T \rangle$ with multiplicity is energy independent

The CMS results are consistent with $x_T=2p_T/\sqrt{s}$ scaling (pQCD prediction) with exponent N=4.9 +- 0.1

Consistent with the hypothesis of limiting fragmentation: production of forward particles is independent on collision energy

Sensitive to the interplay between soft, semi-hard and hard particles production

JHEP 08 (2011) 086
JHEP 01 (2011) 079
EPJC 79 (2019) 391

Long-range correlations

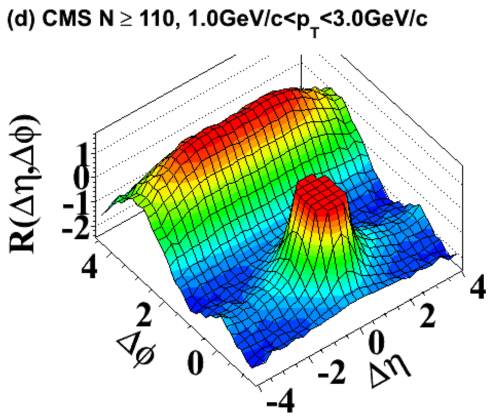

Observed in pp, pPb, PbPb, light AA
CMS, ATLAS, ALICE, RICH
Is not seen in ee, ep, γp (DESY) N_{ch}<40

Qualitatively described effect:
PYTHIA8 string shoving: interacting strings
EPOS LHC:
hydrodynamical evolution
of high-density core (formed by color string fields)

Ridge at $\Delta\phi$~0 and large $\Delta\eta$ at high multiplicity in pp events at intermediate p_T

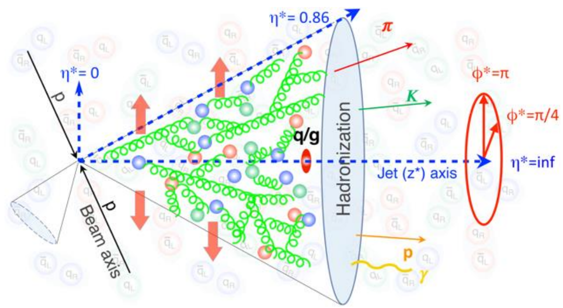

2-particle correlations in jet vs N_{ch}

For N_{ch}>80 hints the collective behaviour

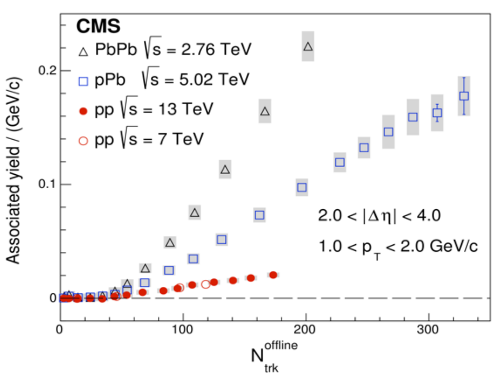

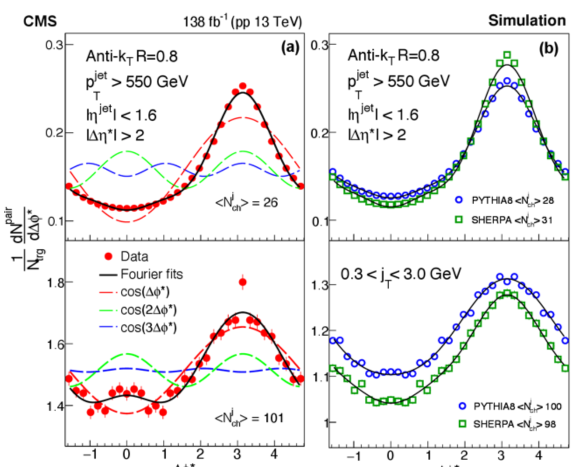

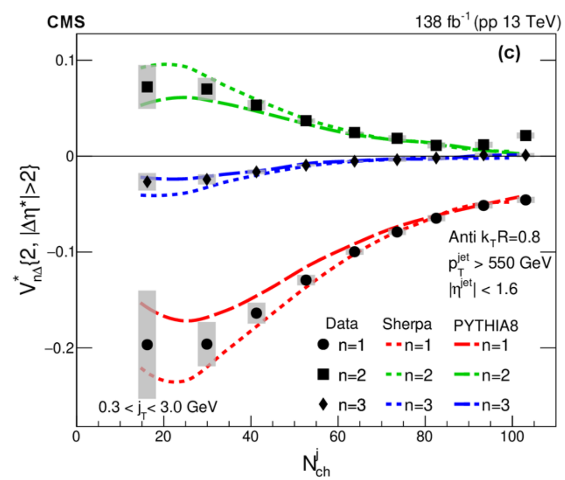

JHEP 09 (2010) 091
PRL 116 (2016) 172302
PRL 133 (2024) 142301

Event shape at 13 TeV

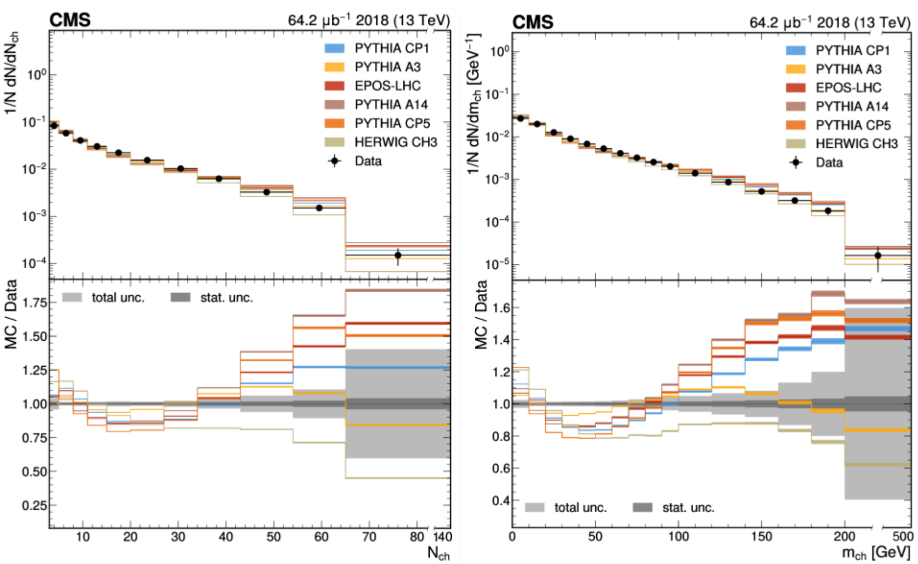

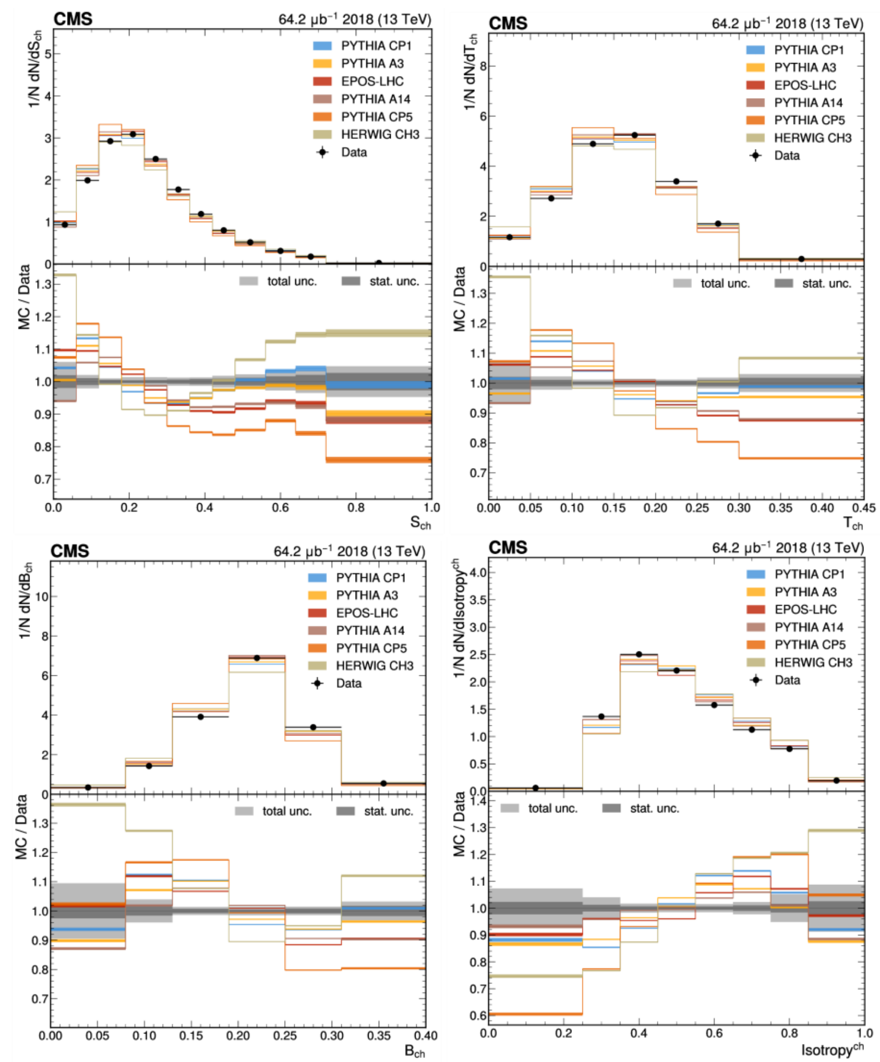

Probing soft and nonperturbative effects

Data prefer more isotropic distributions even within slices of charged-particle multiplicity then simulation

Opposite trend in e+e- (LEP) leads to conclusion that this is initial state effect

[arXiv:2505.17850](https://arxiv.org/abs/2505.17850), **Submitted to PRD**

Hard interactions

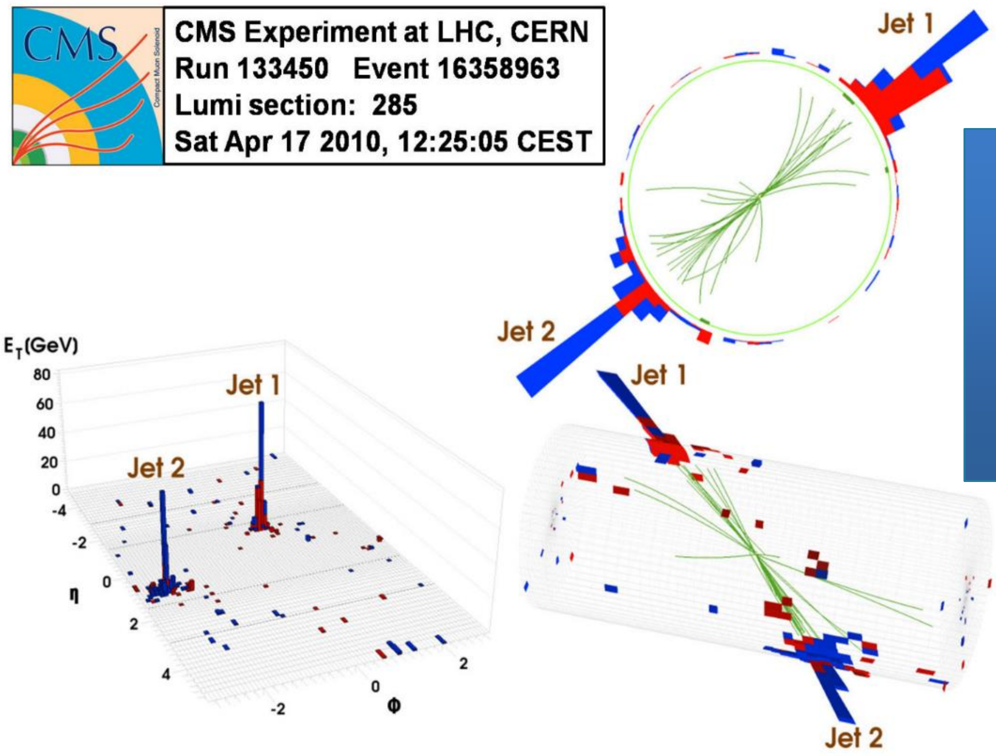

PDFs and α_S measurement
- **DPS**
- **DGLAP vs BFKL**
- **Multijet correlations**

Underlying events

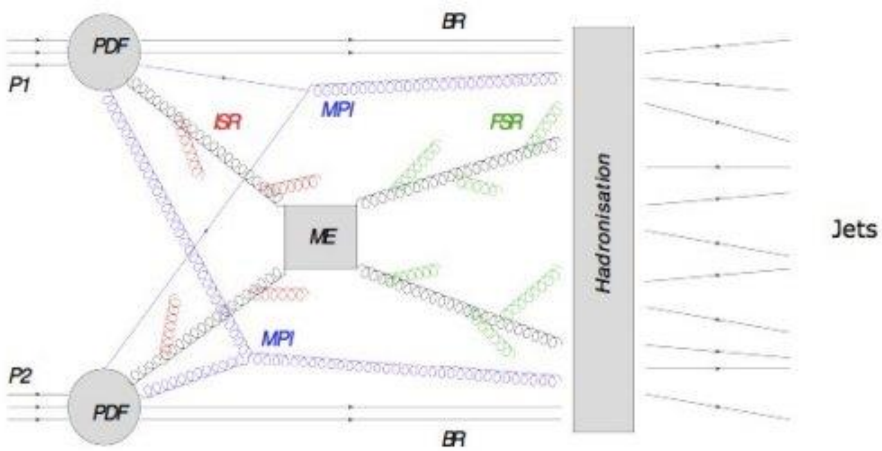

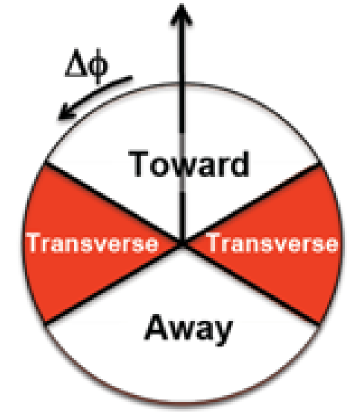

Soft & semi-hard & hard

Beam remnants (BR): everything besides the hard (part of the) interaction, i.e

Initial (ISR) and final (FSR) state radiation

Multiple Parton Interactions (MPI). If higher pt interactions → Double Parton Scattering

UE activity is typically studied in the transverse region in pp collisions as a function of the hard scale of the event, and at different centre-of-mass energies (√s):

Particle production in MinBias events or events with high energy track or jet (hadronic events)

Drell-Yan events, Top events (new)

Underlying events

ttbar events

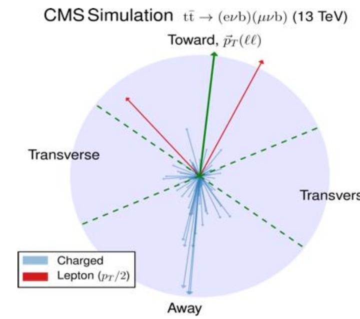

High p_T track
or Tracker jets

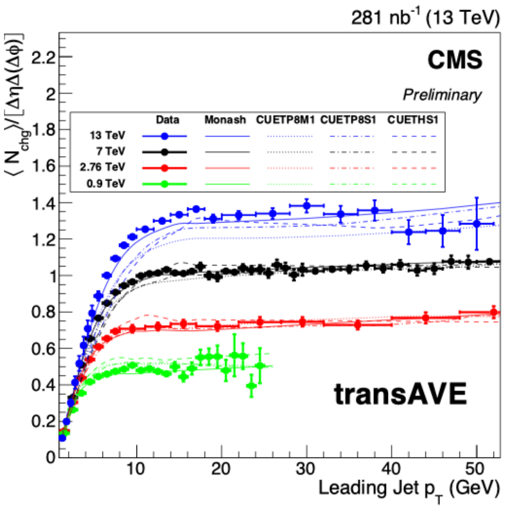

Z+jets

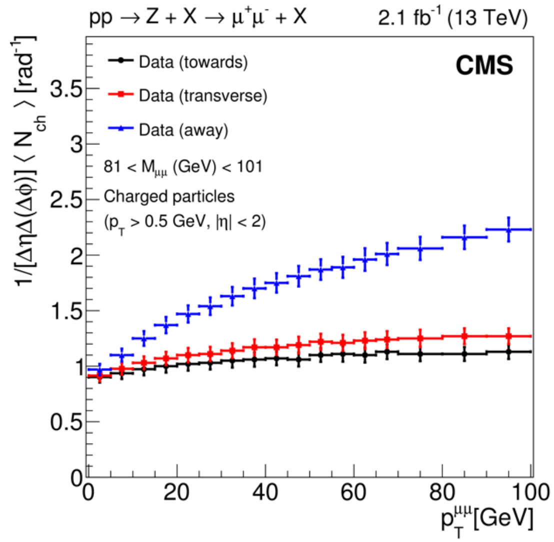

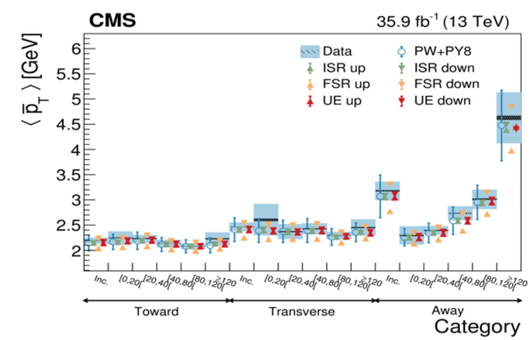

Measurements are used for the UE tunes.

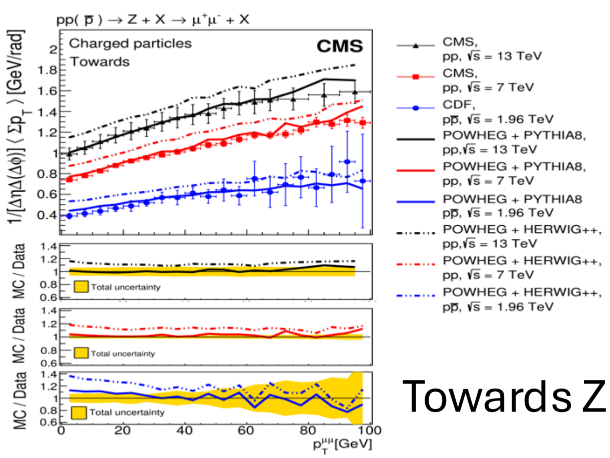

Towards Z

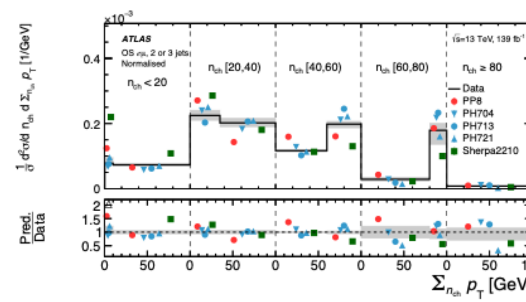

JHEP 07 (2018) 032
EPJC 79 (2019) 123
JHEP 09 (2015) 137
CMS-PAS-FSQ-15-007

Double Parton scattering (DPS)

Two and more hard interactions within the same production vertex can happen.

DPS is characterized by

$$\sigma_{\mathrm{DPS}}^{\mathrm{AB}} = \frac{m}{2}\frac{\sigma_{\mathrm{SPS}}^{A}\sigma_{\mathrm{SPS}}^{B}}{\sigma_{\mathrm{eff}}} \qquad \sigma_{\mathrm{eff}} = \left[\int d^2b\,(T(\mathbf{b}))^2\right]^{-1}$$

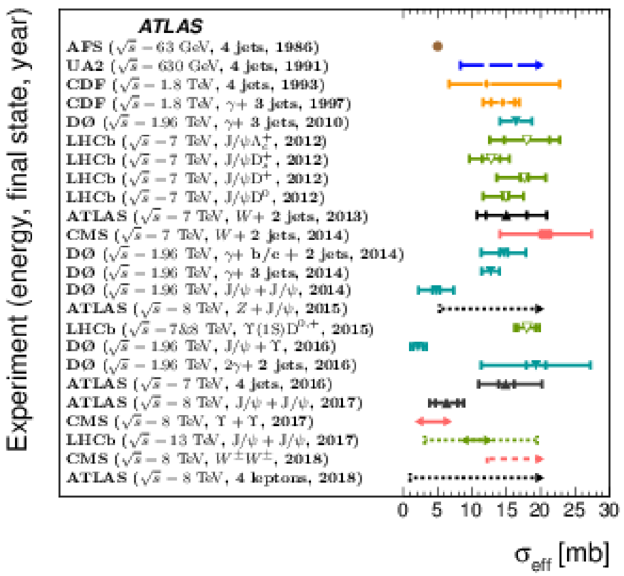

σ_{eff} **is 2-10(10 to 20) mb for g(q)**

T(b) is the overlap function of two interacting hadrons

First observation in same sign WW at 13 TeV (138 fb^{-1}):

[PRL 131 (2023) 091803]

$\sigma_{\mathrm{DPS}}^{\mathrm{WWinc}} = 80.7 \pm 11.2(\mathrm{stat}) + 9.5(\mathrm{syst}) - 8.6(\mathrm{syst}) \pm 12.1(\mathrm{model})$ fb

$\sigma_{\mathrm{DPS}}^{\mathrm{WWfed}} = 6.28 \pm 0.81(\mathrm{stat}) \pm 0.69(\mathrm{syst}) \pm 0.37(\mathrm{model})$ fb

Observed significance = 6.2

$\sigma_{\mathrm{eff}} = 12.2 + 2.9 - 2.2$ **mb**

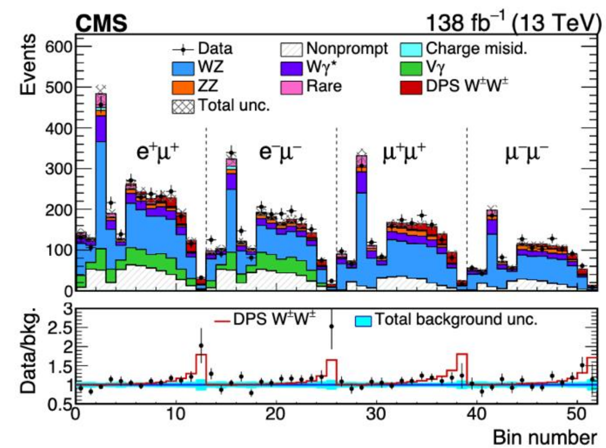

DPS with 4 jets events

[JHEP 01 (2022) 177] **(13 TeV),**

A strong dependence of the extracted values of σ_{eff} on the model used to the describe the SPS contribution is observed.

σ_{eff} = 7-35 mb

σ_{DPS}=15-70 nb

DPS with Z+jets

[JHEP 10 (2021) 176]

Give the additional possibility to constrain MPI models

PDFs and α_s

For the fixed pQCD order and definite PDF evolution (DGLAP, BFKL, CCFM,..):
A) Define PDFs at fixed α_s
B) Define α_s for the particulary PDF set which gives the best approximation of the Data by Theory
C) Combined PDFs and α_s fit

Process	Sensitivity
W mass measurement	Valence quarks
W,Z production	Quark flavor separation
W+c production	Strange quark
Drell-Yan, high mass	Sea quark, high-x, photon PDF
Drell-Yan low mass	Low-x, resummation
W,Z+jets	Gluon medium-x
Inclusive jets, multijets	Gluon and $\alpha_s(M_Z)$
Direct photon	Gluon medium, high-x
ttbar, single top	Gluon, $\alpha_s(M_Z)$

Differential production (single, double, triple), correlations, ratios, asymmetry

Jet production: sensitivity to g-PDF and to α_S

CMS, 13 TeV, Integrated luminosity 36.3 fb^{-1}

Comparison with NNLO

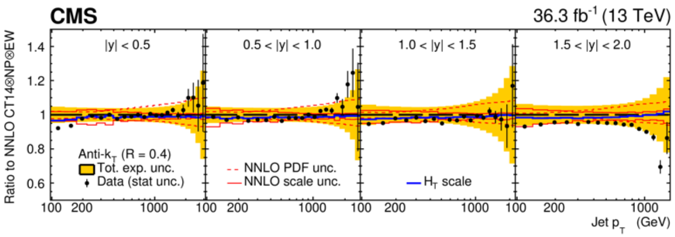

Comparison with NLO+NLL

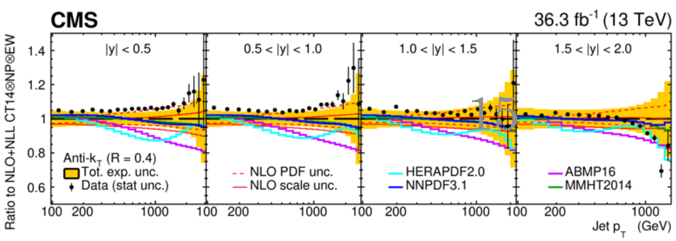

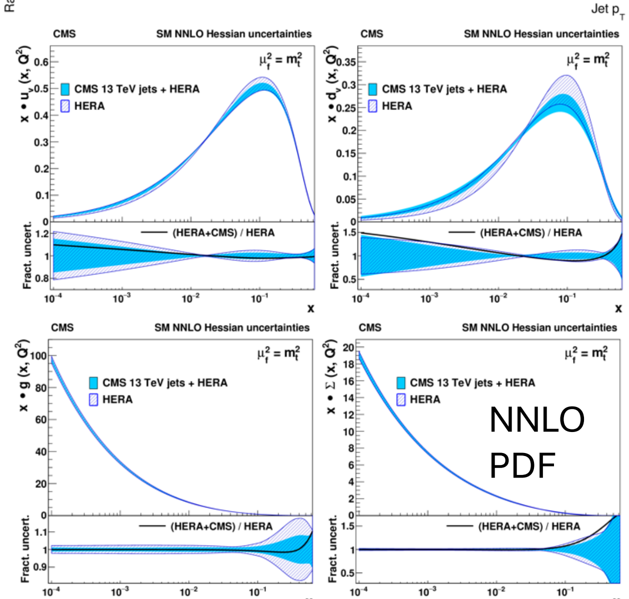

NNLO PDF

Double-differential inclusive jet production + HERA DIS + the normalized triple-differential ttbar cross-section, DGLAP evolution PDF and $\alpha_S(M_Z)$ = 0.1166+-0.0017 at NNLO (approximated by k from NLO), uncertainties comparable with world average PDF at NLO extracted simultaneously with Wilson coefficient in EFT (SMEFT)

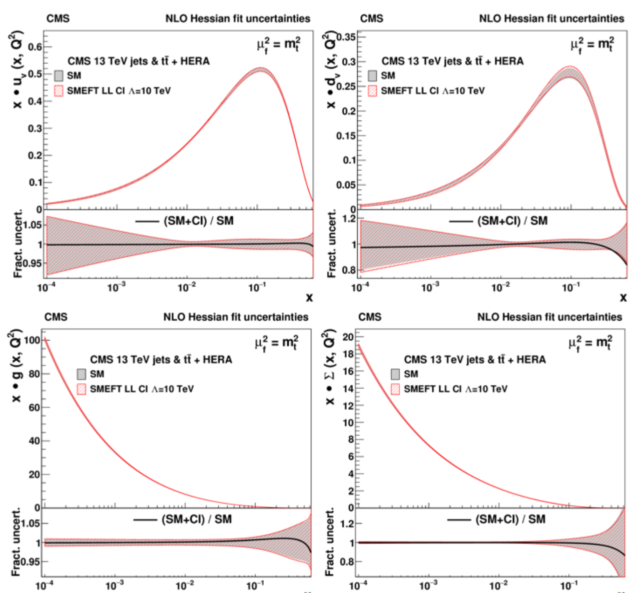

NLO PDF with Contact Interactions

No evidence for Contact Interactions:
95% confidence level exclusion limit for the left-handed model with constructive Interference
Λ > 24 TeV

JHEP 02 (2022) 142 [Addendum]

Determination of α_S and it's running at NNLO accuracy with inclusive jet production

Double differential jet production, p_T, y combined with HERA DIS
CMS inclusive jets at 2.76 + 7 + 8 + 13 TeV
Theory modelling: NNLO pQCD, 5 flavors, leading colour and leading-flavour-number approximations with NNLOJET program
Factorization and renormalization scales are set to the individual jet p_T
Cross-section predictions in p_T,y bin are done in APPLFAST format, EW corrections at NLO
DGLAP evolution equations at NNLO in pQCD (QCDNUM)

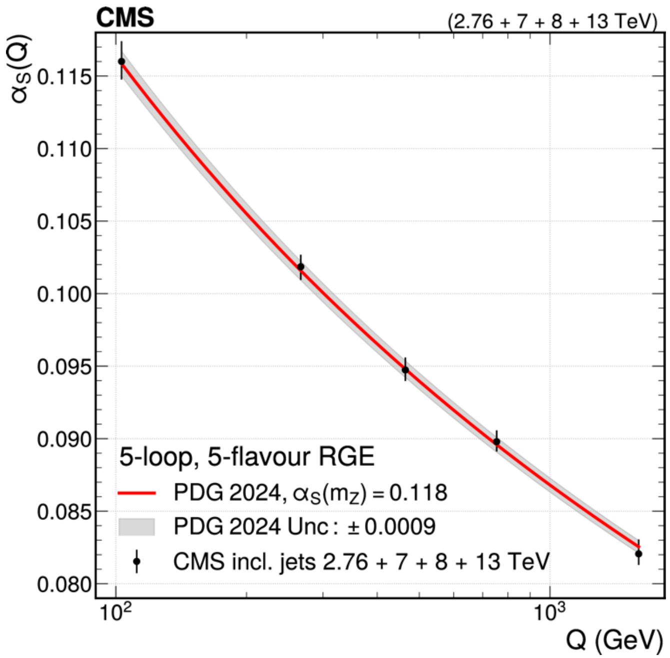

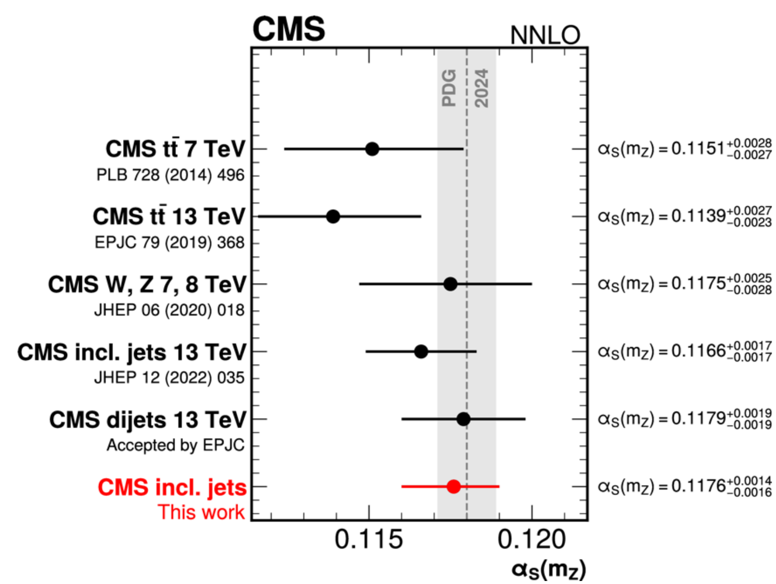

$\alpha_S(m_Z) = 0.1176^{+0.0014}_{-0.0016}$

PLB 868 (2025) 139651

DiJet production: sensitivity to g-PDF and to α_S

Both 2D ($|y_{max}|$,m_{dijet}) and 3D ($y* = |y1 - y2|/2$, $yb = |y1 + y2|/2$, m_{dijet}/p_{Tdijet}) measurements are performed as a function of the kinematic properties of the two jets with the highest p_T in the event. Fixed-order theoretical predictions at NNLO (NNLOJET)

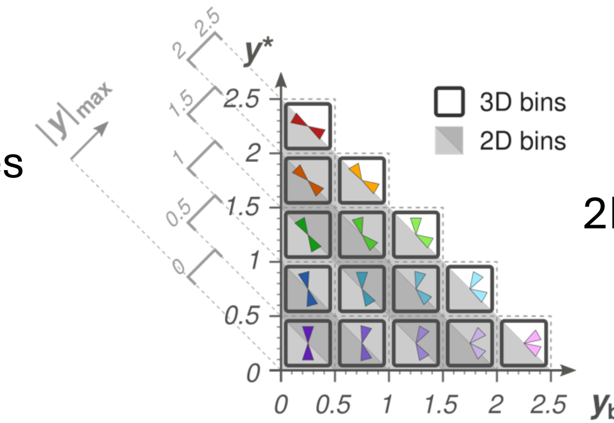

2D vs 3D

Jets: antiKT, R=0.4,0.8

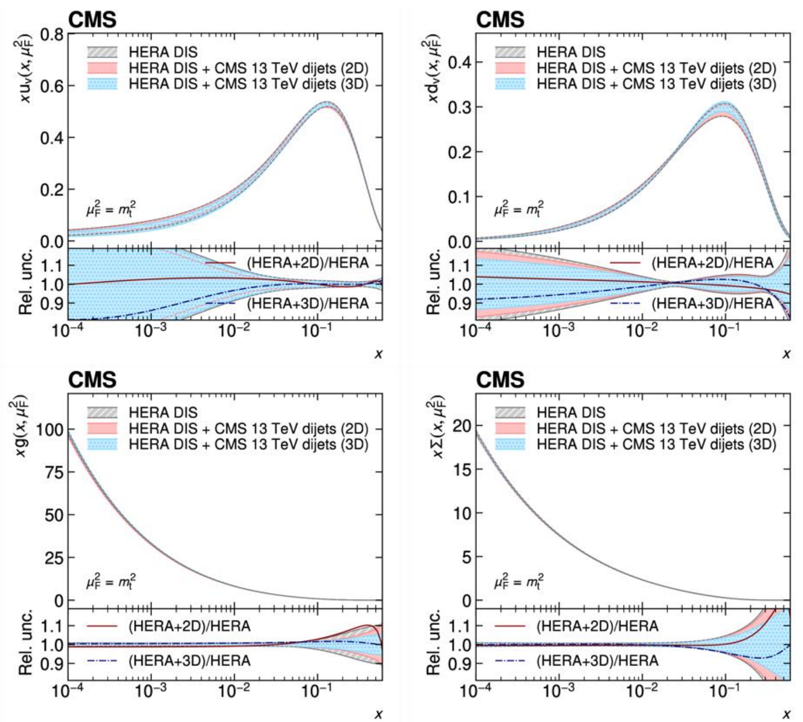

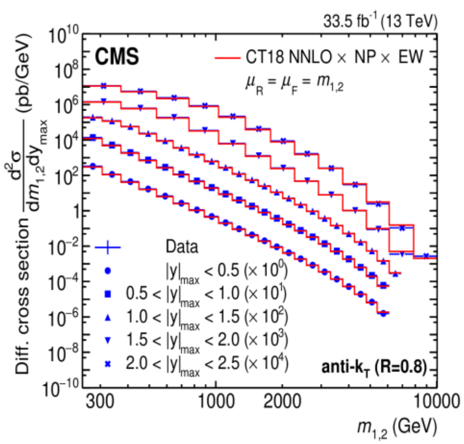

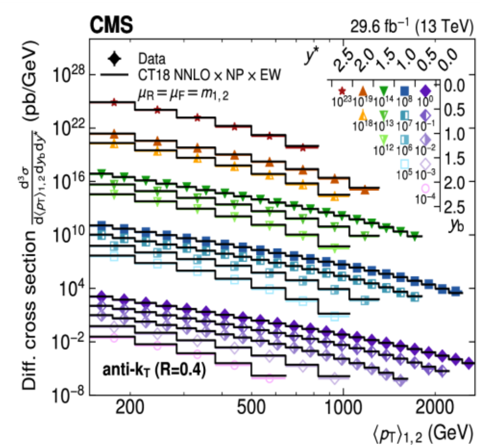

2D: $\alpha_S(m_Z)=0.1179 \pm 0.0019$ (total)
3D: $\alpha_S(m_Z)= 0.1181 \pm 0.0022$ (total)

EPJC 85 (2025) 72

Multijets correlation and strong couplings

RGE predicts the $a_S(Q)$ dependence but not the absolute value **134 fb^{-1}**

Azimuthal correlations in >=3jets events, leading jet p_T = 360–3170 GeV, |y|<2.5

Neighboring jet with p_T>100 GeV; angle conditions

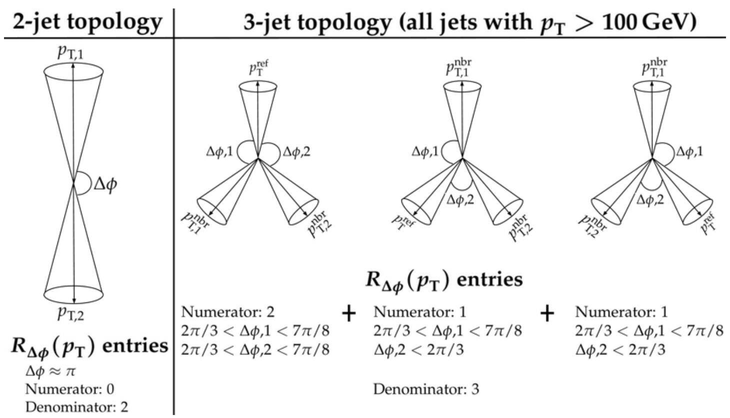

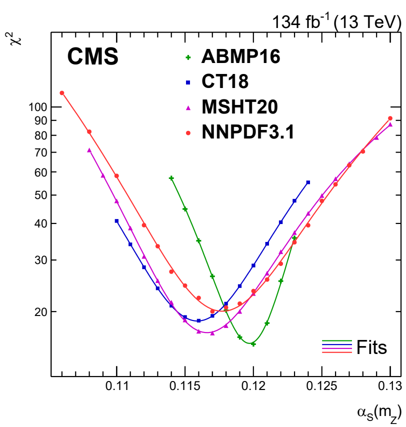

$$R_{\Delta\phi}(p_T) = \frac{\sum_{n=0}^{\infty} nN(p_T, n)}{\sum_{n=0}^{\infty} N(p_T, n)} \sim a_S$$

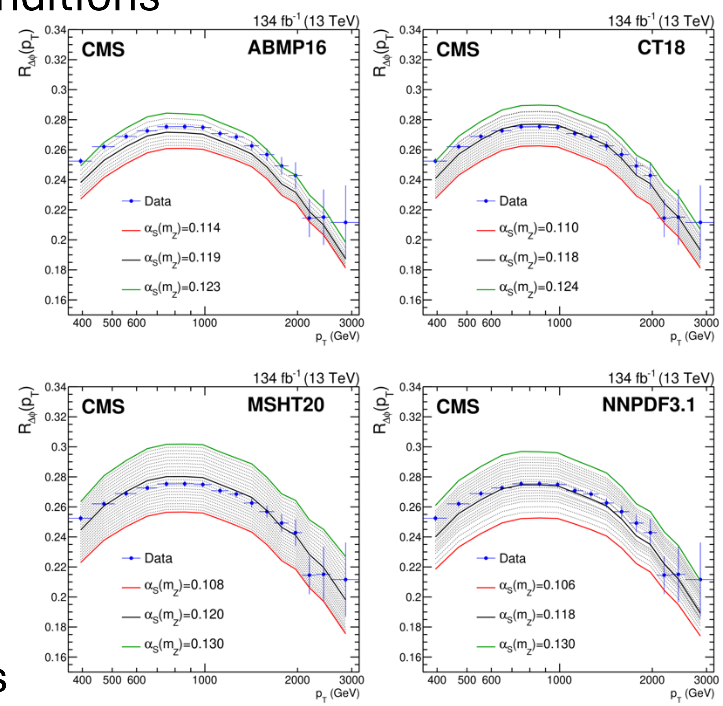

Vary a_S for each PDF s

$a_S(M_Z)$=0.1177+-0.0013(exp)+0.0116-0.0073(th) at NLO accuracy

EPJC 84 (2024) 842

Energy correlators, evolution equation and strong couplings

The NLO + NNLL$_{approx}$ theoretical predictions are corrected to hadron-level and normalized to the measured data.

The different x_L regions provide information on the dynamics of jet formation, so that one can examine the DGLAP equations.

In QCD calculations:

E3C/E2C~$\alpha_S \ln(x_L)$

E3C=$\sum_{i,j,k}^{n} d\sigma \frac{E_i E_j E_k}{E^3} \delta(x_L - \max(\Delta R_{i,j}, \Delta R_{i,k}, \Delta R_{k,j}))$

E2C=$\sum_{i,j}^{n} d\sigma \frac{E_i E_j}{E^2} \delta(x_L - \Delta R_{i,j})$

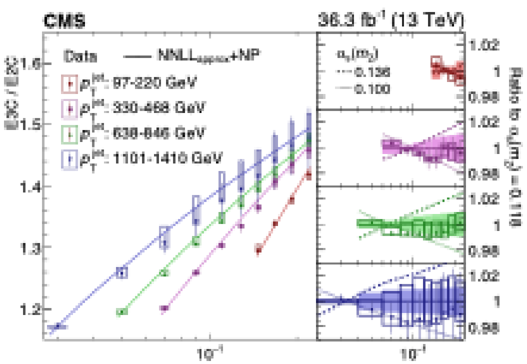

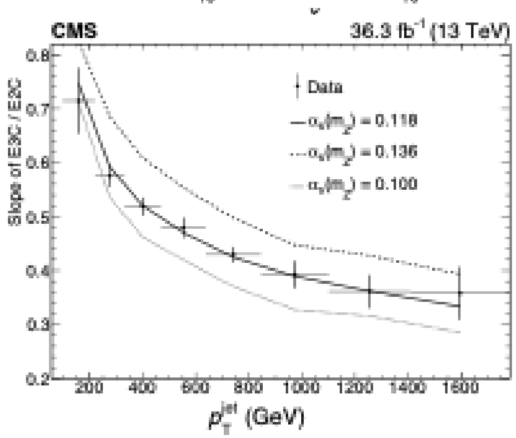

x_L-maximum distance between pair of particles.

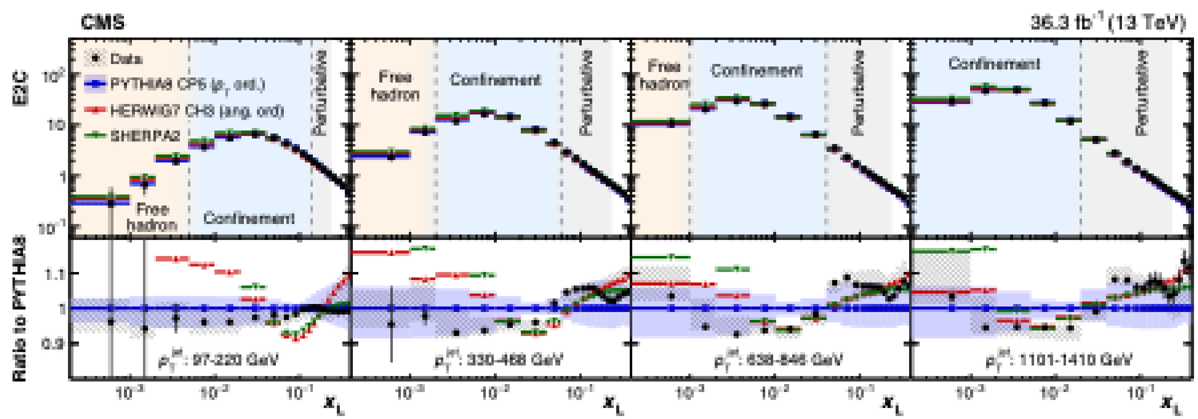

$a_S(M_Z)=0.1229^{+0.0014}_{-0.012}(stat)^{+0.003}_{-0.0033}(theo)^{+0.0023}_{-0.0036}(exp)$

[PRL 133 (2024) 071903](#)

Summary on α_S

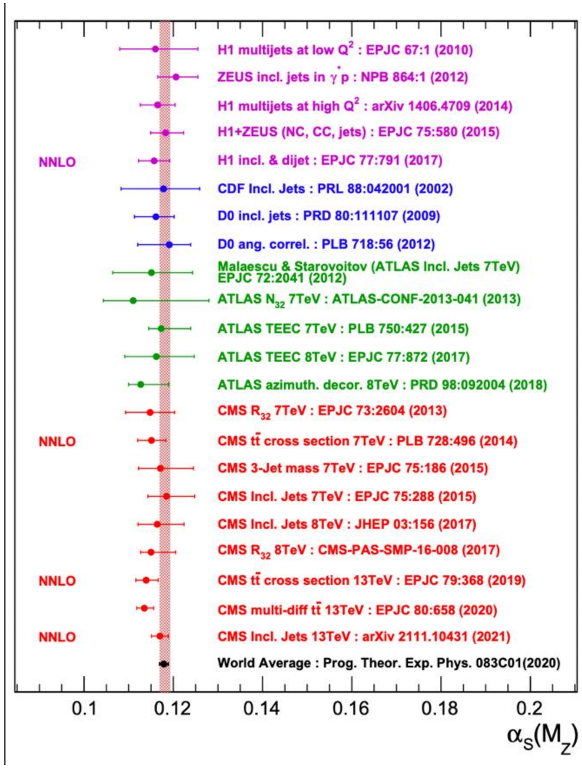

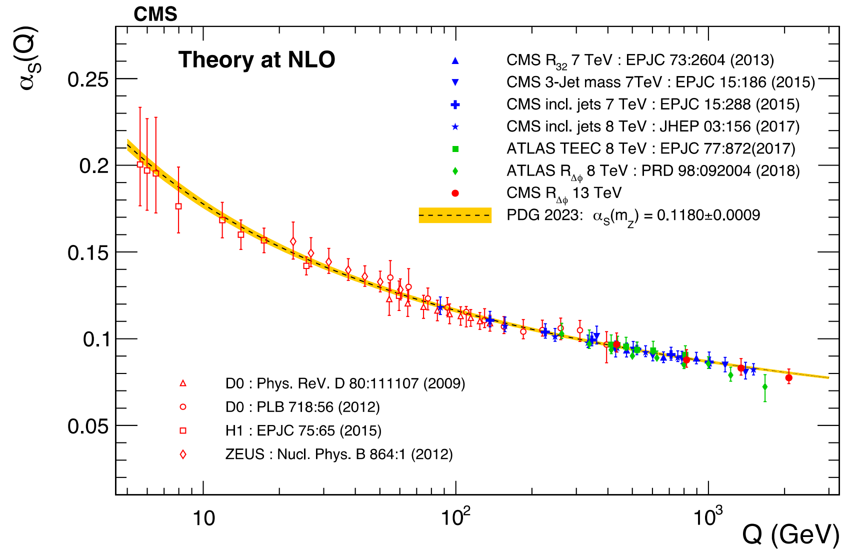

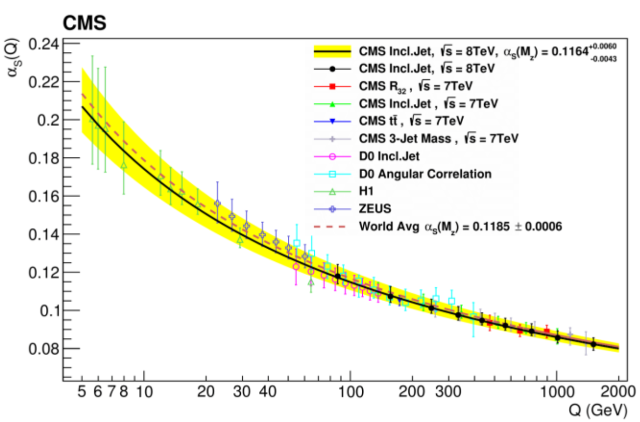

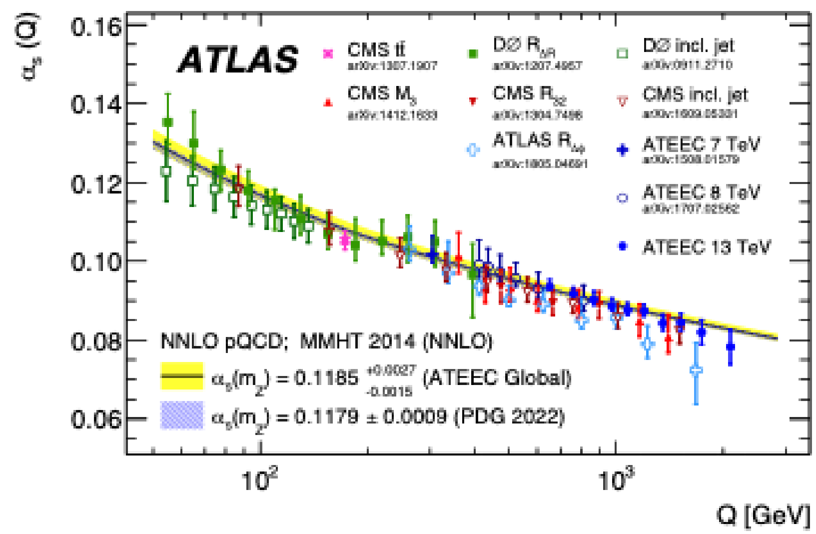

W+c: strange quark PDF

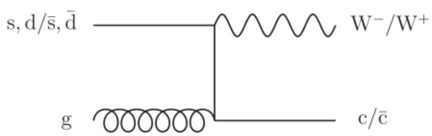

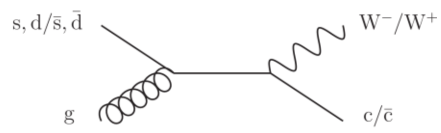

sg->W+c dominant contribution
->strange quark PDF and
$s - \bar{s}$ PDF asymmetry

$$R_s = \frac{s + \bar{s}}{\bar{u} + \bar{d}}$$

Sensitive to $s - \bar{s}$ asymmetry and to down $q - anti\ q$ asymmetry due-to Cabibbo-suppressed d-quark in the W + c production.

$p_T^l > 35$ GeV, $|\eta^l|<2.4$, $p_T^{c\text{-jet}}>30$ GeV
$|\eta^{c\text{-jet}}|<2.4$
Measured and unfolded to particle level
σ(W + c) = 148.7 ± 0.4 (stat) ± 5.6 (syst) pb

MCFM NLO

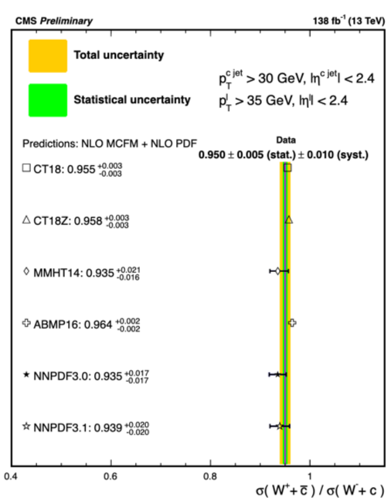

CMPP, NNLO QCD+
NLO EW

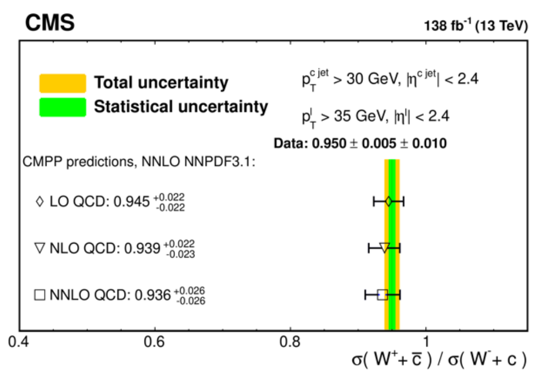

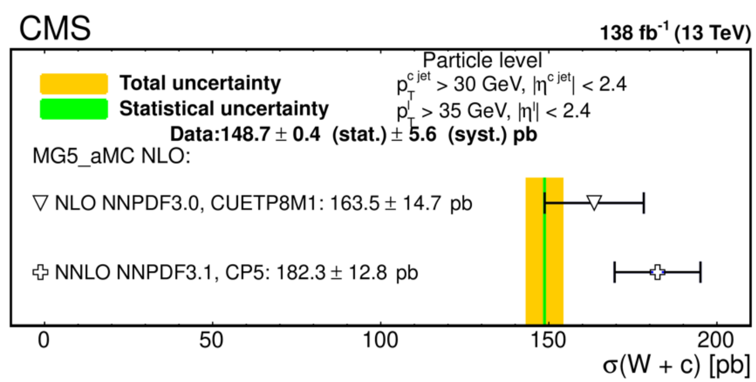

At parton level
σ(W + c) = 163.4 ± 0.5 (stat) ± 6.2 (syst) pb

[EPJC 84 (2024) 27]

$s - \bar{s}$ assymetry in Data
$0.95 \pm 0.005(stat) \pm 0.010(syst)$

Z+c: towards c-PDFs (towards c-PDF)

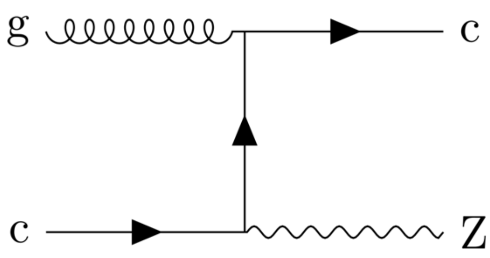

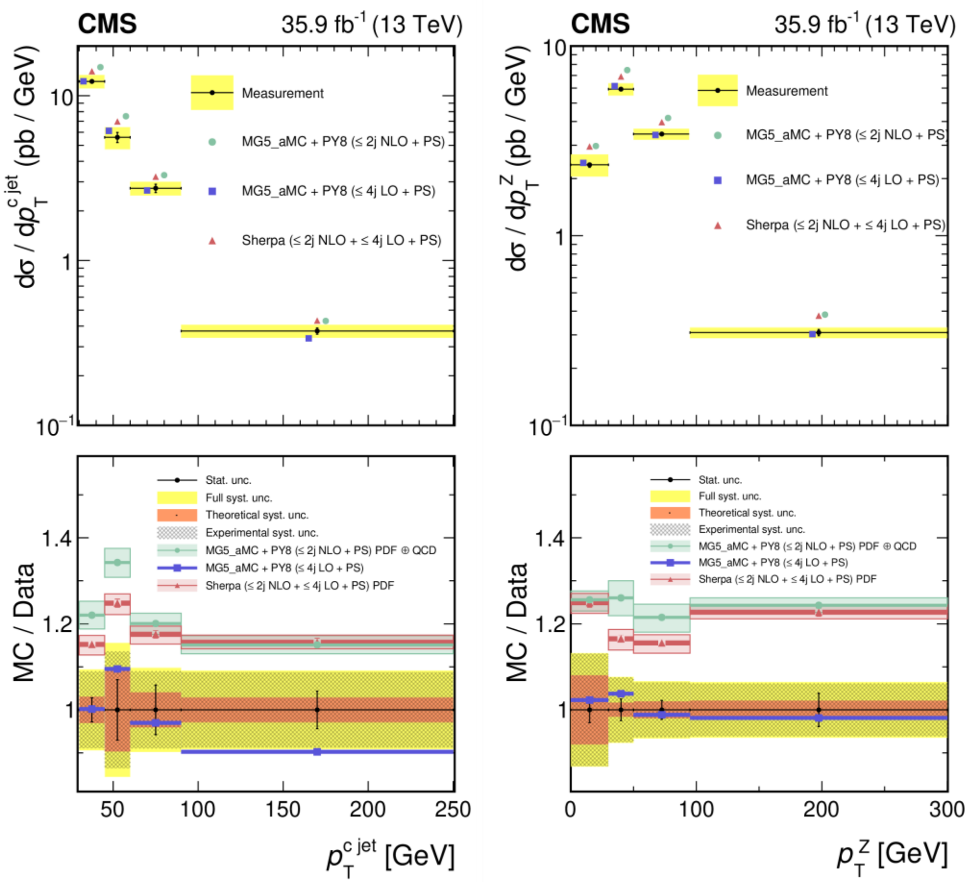

MCatNLO 2.2.2 and Sherpa 2.2 overestimate Z+c cross-section at NLO and aMCatNLO agreed with data at LO.
FxFx for NLO, MLM for LO
Cross-sections are normalized to NNLO with FEWZ 3.1.
NNPDF3.0

Inclusive Z+c cross-section:
405.4 ± 5.6 (stat)
± 24.3 (exp)
± 3.7 (theo) pb
MadGraph5+MCatNLO:
524.9 ± 11.7 (theo) pb

JHEP 04 (2021) 109

Z+b: towards b-quarks PDFs and 4 vs 5-flavor schema

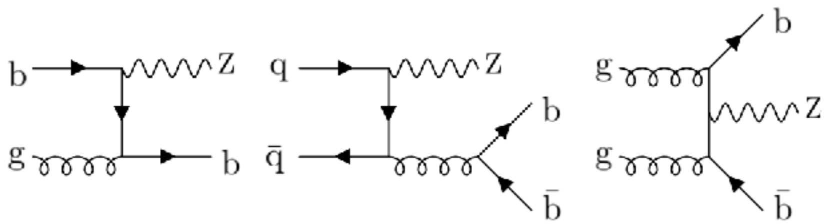

Current simulations are in NLO either in 4 or 5 FNS.
In 4 FNS b-quark does not contribute to PDF.
Massive b through gluon splitting
In 5 FNS b-quark typically massless but b contributes to PDF

CMS 137fb^{-1}
$|p_T|>35$ GeV, $p_T^{sublead}>25$ GeV
$|\eta|<2.4$, $M_Z=[71\text{-}111]$ GeV
Generator b-jet $p_T>30$ GeV, $|\eta|<2.4$

Normalized to fiducial Cross-section

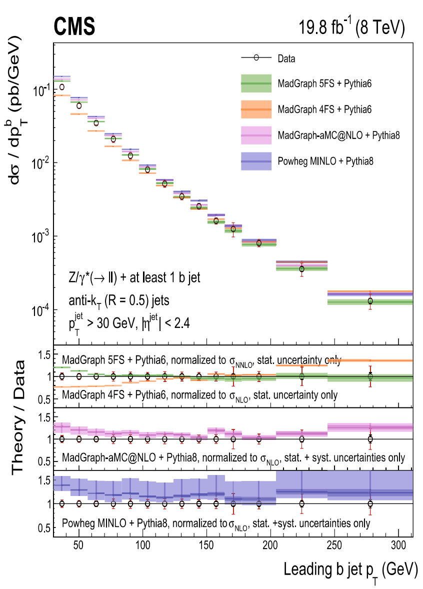

$\sigma_{fid}(Z+>=1b) = 6.52 \pm 0.04 \pm 0.4 \pm 0.014$ pb

$\sigma_{fid}(Z+>=2b) = 0.65 \pm 0.03 \pm 0.07 \pm 0.02$ pb

PRD 105 (2022) 092014
EPJC 77 (2017) 751

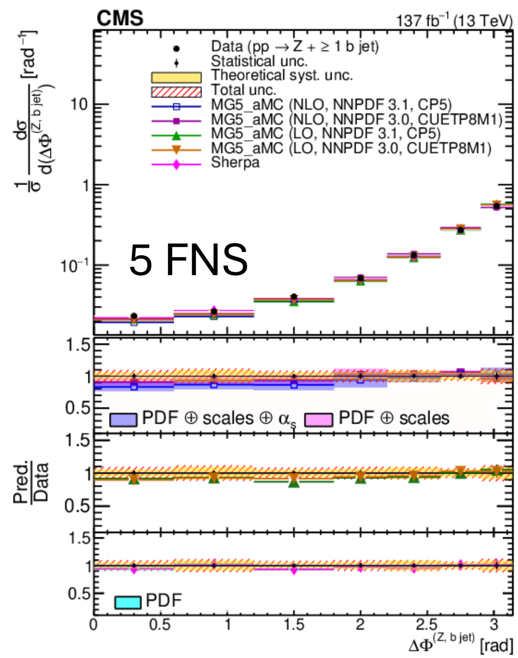

Jet substructure and Lund plane

Reclustering with CA algo.

$$k_t = p_T^{\text{emission}} \cdot \Delta R(p^{\text{emission}}, p^{\text{core}})$$

$$\Delta R = \sqrt{(y^{j1} - y^{j2})^2 + (\varphi^{j1} - \varphi^{j2})^2}$$

$$\rho(k_T, \Delta R) = \frac{1}{N_{\text{jets}}} \frac{d^2 N_{\text{emissions}}}{d\ln\left(\frac{k_T}{\text{GeV}}\right) d\ln(R/\Delta R)} \approx \frac{2}{\pi} C_R \alpha_S(k_T)$$

Jets with $p_T > 700$ GeV

$|y| < 1.7$

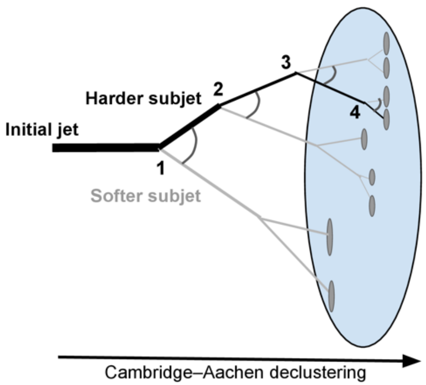

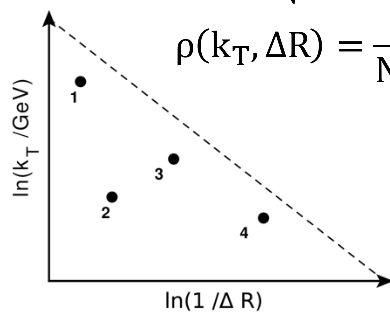

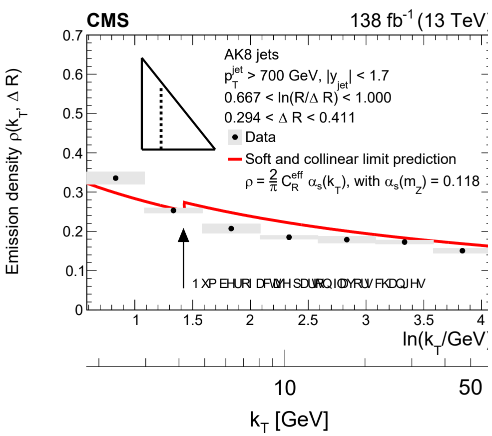

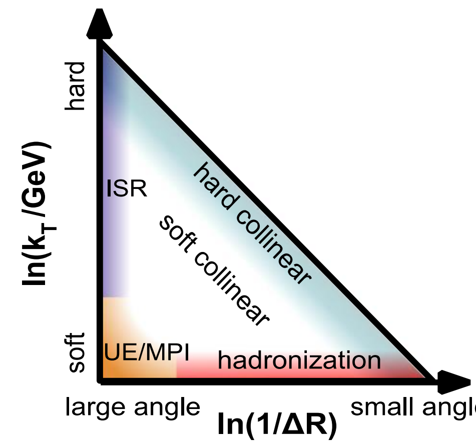

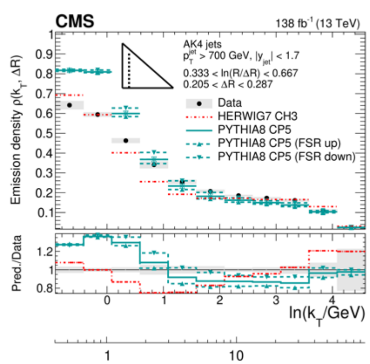

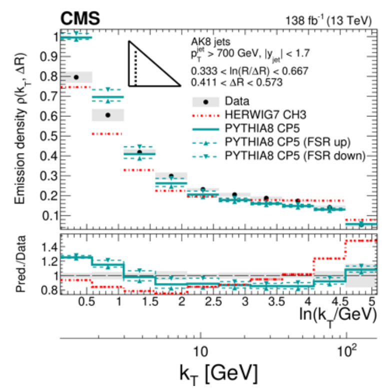

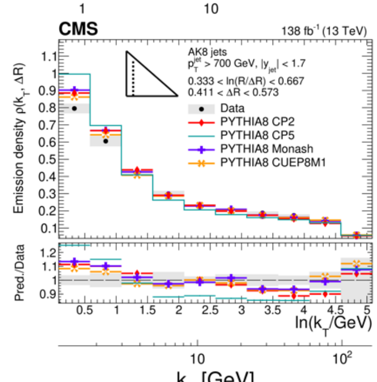

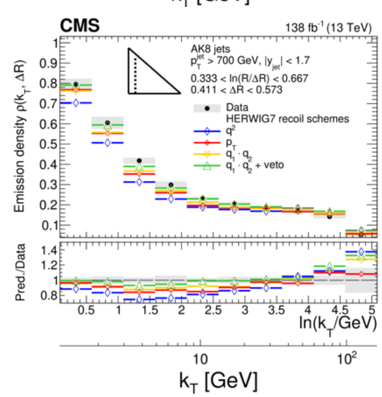

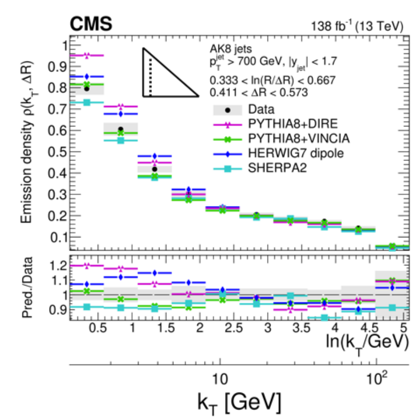

Rise of the density is consistent with running $\alpha_S(k_T)$.

JHEP 05 (2024) 116

Angular distance and momentum ratio for 3 high-p_T objects

- Matrix element expansion and parton shower
  Multi-parton interactions and
- hadronization

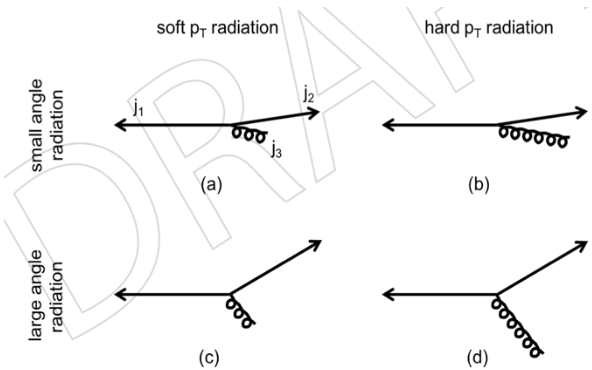

Three-jet events	
Transverse momentum of the leading jet (j_1)	$p_{T1} > 510\,\text{GeV}$
Transverse momentum of each jet and rapidity of $j_{1,2}$	$p_T > 30\,\text{GeV}$, $\lvert y_{1,2}\rvert < 2.5$
Azimuthal angle difference between j_1 and j_2	$\pi - 1 < \Delta\phi_{12} < \pi$
Transverse momentum ratio between j_2 and j_3	$0.1 < p_{T3}/p_{T2} < 0.9$
Angular distance between j_2 and j_3	$R_{jet} + 0.1 < \Delta R_{23} < 1.5$
Number of selected events at $\sqrt{s} = 8\,(13)$ TeV	777 618 (613 254)
Z + two-jet events	
Transverse momentum of the Z boson (j_1)	$p_{T1} > 80\,\text{GeV}$, $\lvert y_1\rvert < 2$
Transverse momentum and rapidity of j_2	$p_{T2} > 80\,\text{GeV}$, $\lvert y_2\rvert < 1$
Transverse momentum and rapidity of j_3	$p_{T3} > 20\,\text{GeV}$, $\lvert y_3\rvert < 2.4$
Azimuthal angle difference between Z and j_2	$2 < \lvert\Delta\phi_{12}\rvert < \pi$
Dimuon mass	$70 < m_{\mu^+\mu^-} < 110\,\text{GeV}$
Angular distance between j_3 and j_2	$0.5 < \Delta R_{23} < 1.5$
Number of selected events	15 466

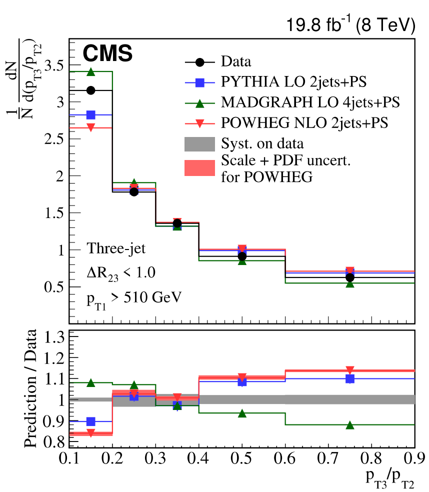

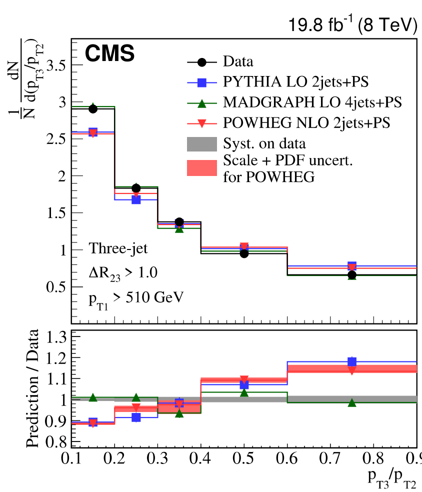

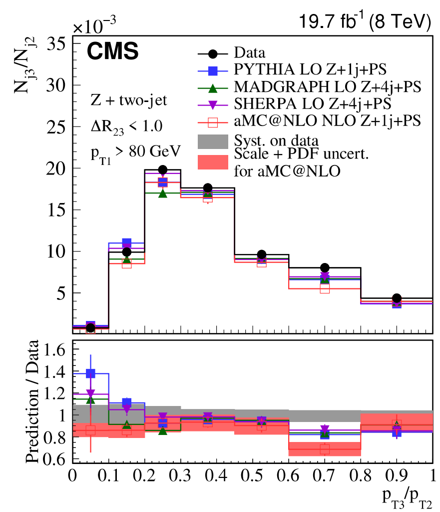

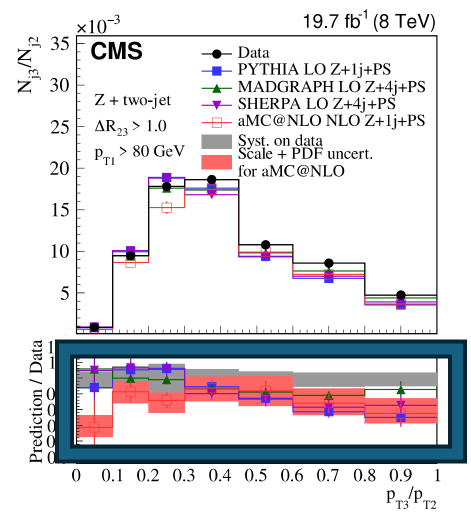

Partially compensated by ttbar and VV processes

EPJC 81 (2021) 852

Azimuthal correlations in Z+jets at 13 TeV

Table 2: Particle-level phase space definition

object	requirement
leading (subleading) lepton	$p_T > 25(20)$ GeV, $\lvert\eta\rvert < 2.4$
lepton-jet separation	$\Delta R_{\ell,j} > 0.4$
lepton pair mass	$76 < m_{\ell^+\ell^-} < 106$ GeV
jet	$p_T > 30$ GeV, $\lvert\eta_{jet}\rvert < 2.4$

$\Delta R(l,j)>0.4$

$p_T^Z<10$ GeV , $p_T^{jet}>30$ GEV, $|y_{jet}|<2.4$

30 GeV$<p_T^Z<50$ GeV, $p_T^{jet}>30$ GEV , $|y_{jet}|<2.4$

$p_T^Z>100$ GeV , $p_T^{jet}>30$ GEV , $|y_{jet}|<2.4$

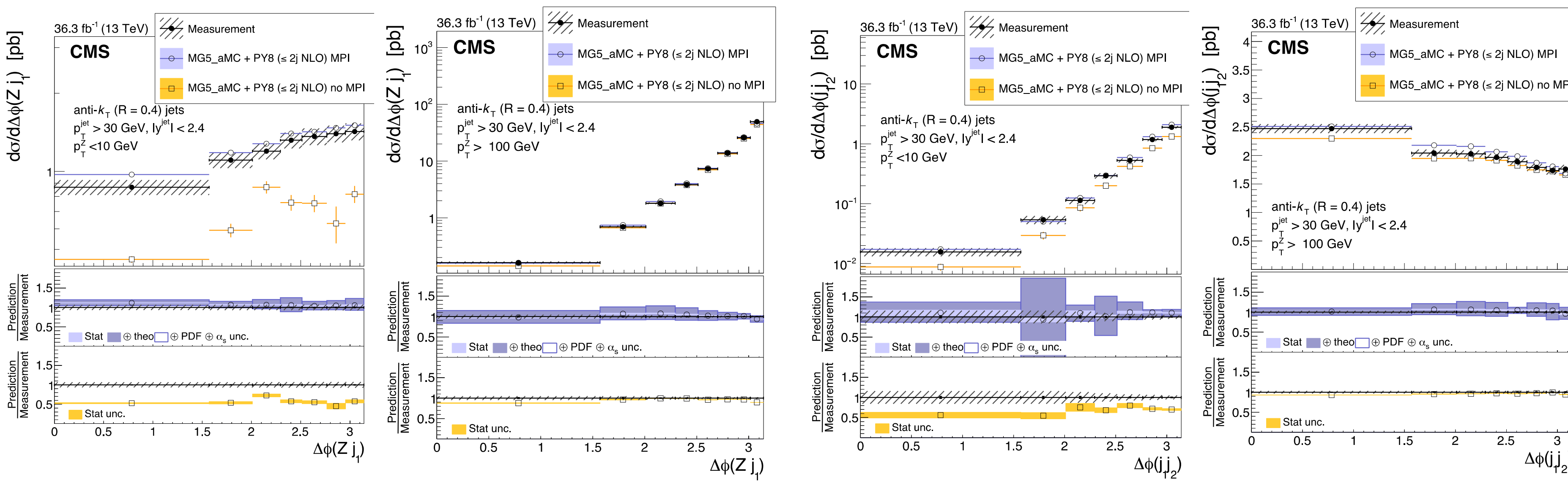

Z at Low p_T with high p_T jet (~1% of events has high p_T jet) is emitted from high p_T jet (EWK correction)

Z at high p_T with jets: Z+jets is the dominant process

EPJC 83 (2023) 722

Observation of WZγ production and constraints on new physics scenarios

Multiboson production processes are sensitive to contributions with triple gauge couplings
(TGCs) and quartic gauge couplings (QGCs).

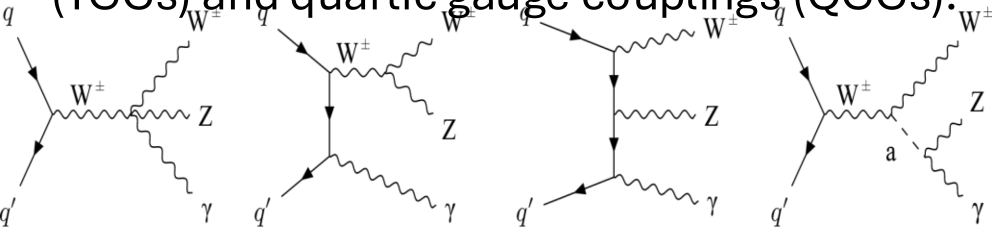

A search for an axion-like particle (ALP) predicted by the Peccei–Quinn solution of the strong CP problem in QCD.

Limits on anomalous quartic gauge couplings (SMEFT – 8 operators)
The presence of nonzero aQGCs would enhance the production of events with large WZγ mass.
No significant excess of events with respect to the SM prediction is observed.

WZγ production:
significance=5.4(expected); 3.8 (observed).
σSM = 5.48 ± 1.11 fb compatible with SM prediction 3.69 ± 0.15 (PDF) ± 0.19 (scale) fb

Limits on photophobic axion-like particle

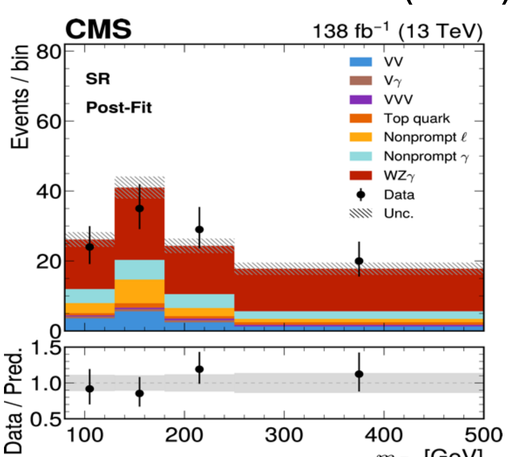

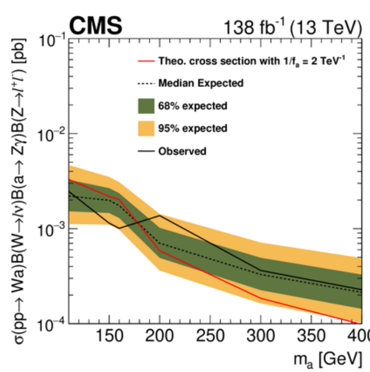

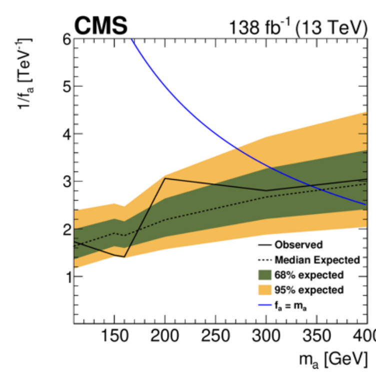

PRD 112 (2025) 012009

Summary

- **CMS measures both hard and soft QCD processes in various phase space regions and compare them with a wide range of LO , NLO and NNLO calculations**
- **CMS measurements are used for the combinations with other experiments in global fits and in Monte-Carlo Models tuning. Validation of the QCD predictions (scaling properties, particles spectra, strong coupling behavior, PDFs, evolution, etc) allows to further constrain and tune existing models.**

More results can be found in CMS public web page:

http://cms-results.web.cern.ch/cms-results/public-results/publications/SMP/index.html

http://cms-results.web.cern.ch/cms-results/public-results/publications/FSQ/index.html

Back-up

Charged particles

new input to the dynamics of soft hadronic interactions: interplay between soft and hard processes: no one MC describes data in all configurations

p_T>500 MeV, |η|<2.4

change of the slope at n~20

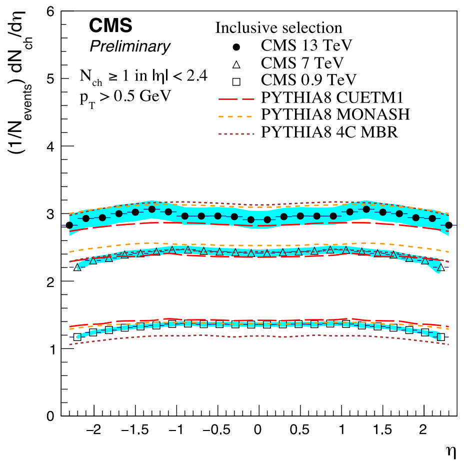

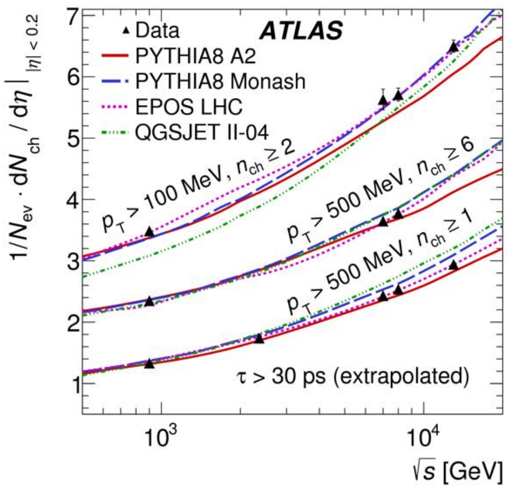

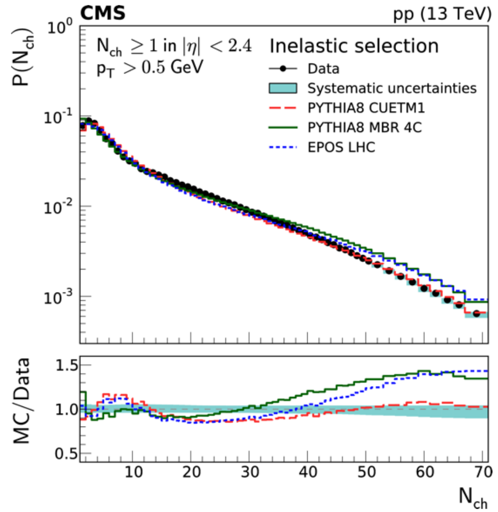

p_T>0 MeV, |η|<0.5

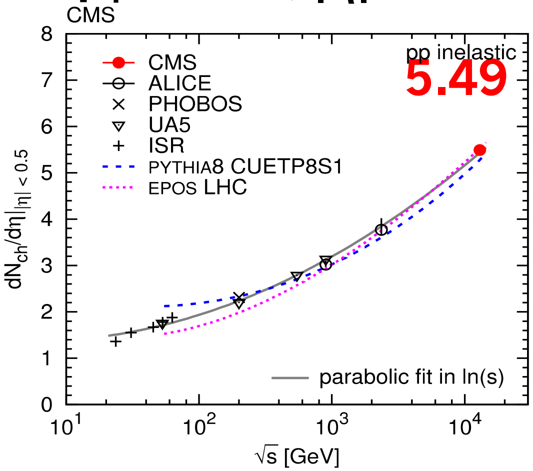

CMS-PAS-FSQ-15-008
EPJC 78 (2018) 697
PLB 751(2015)143
JHEP 01 (2011) 079
EPJC 76(2016) 502
EPJC 81(2021) 630

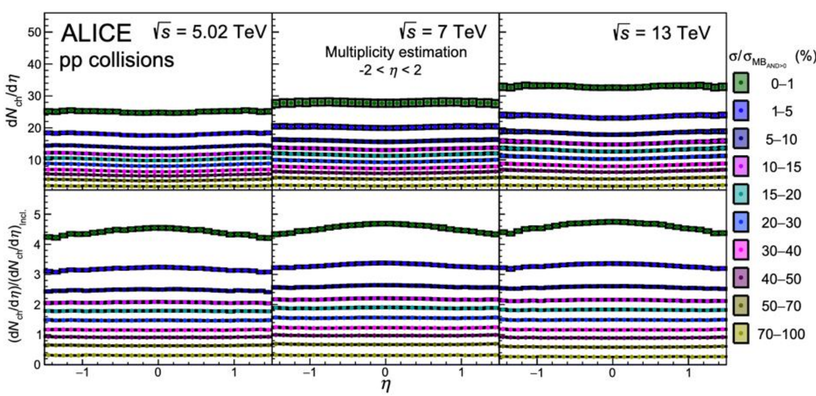

W+-, Z production and α_S

Sensitive to $\alpha_S(m_Z)$ due-to ISR, virtual gluon exchange, gq scattering (NLO, NNLO, ...). Calculate V-production cross-section at NNLO level varying $\alpha_S(m_Z)$ and compare theoretical predictions to experimental data (12 samples with different decay modes).

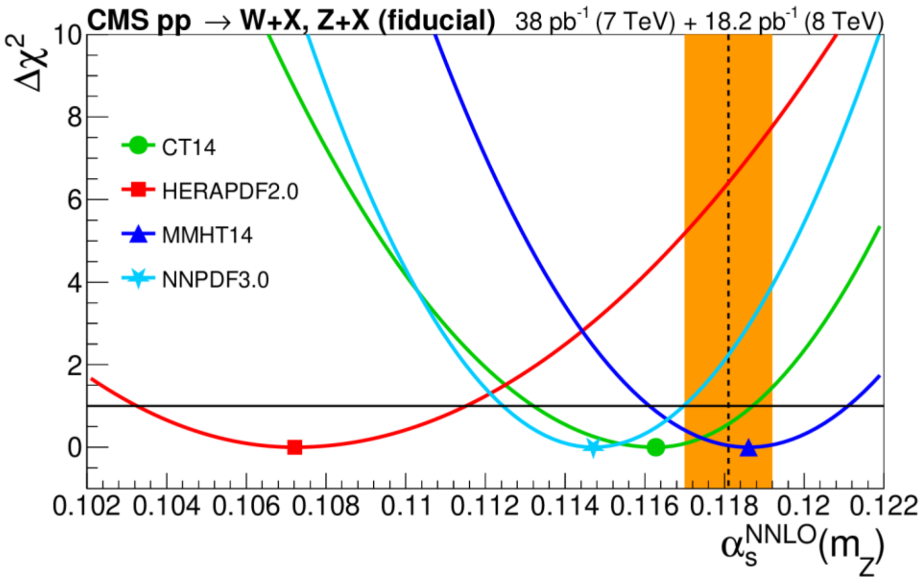

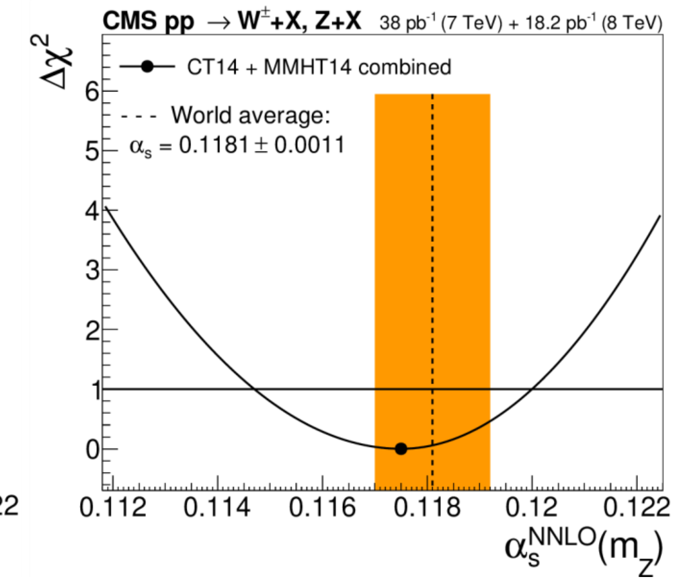

Cross-sections with CT14 and MMHT14 sets are the most sensitive to the α_S value. Robust and stable with respect to variations in the data and theoretical cross sections.

$\alpha_S = 0.1163^{+0.0024}_{-0.0031}$ (CT14) or $0.1072^{+0.0043}_{-0.0040}$ (HERAPDF2.0) or $0.1186^{+0.0025}_{-0.0025}$ (MMHT14) or $0.1147^{+0.0023}_{-0.0023}$ (NNPDF3.0)

The result derived combining the CT14 and MMHT14 extractions:

$$\alpha_S = 0.1175^{+0.0025}_{-0.0028}$$

This extracted value is fully compatible with the current world average.

CMS:JHEP 06 (2020) 018

Jet multiplicity and jet pt in multijet events

Transverse momentum dependent (TMD) PDF
Probability branching method (PB)

Jet selections: |y|<2.5
p_T^{j1}>200 GeV, p_T^{j2}>100 GeV
p_T^{j3}>50 GeV

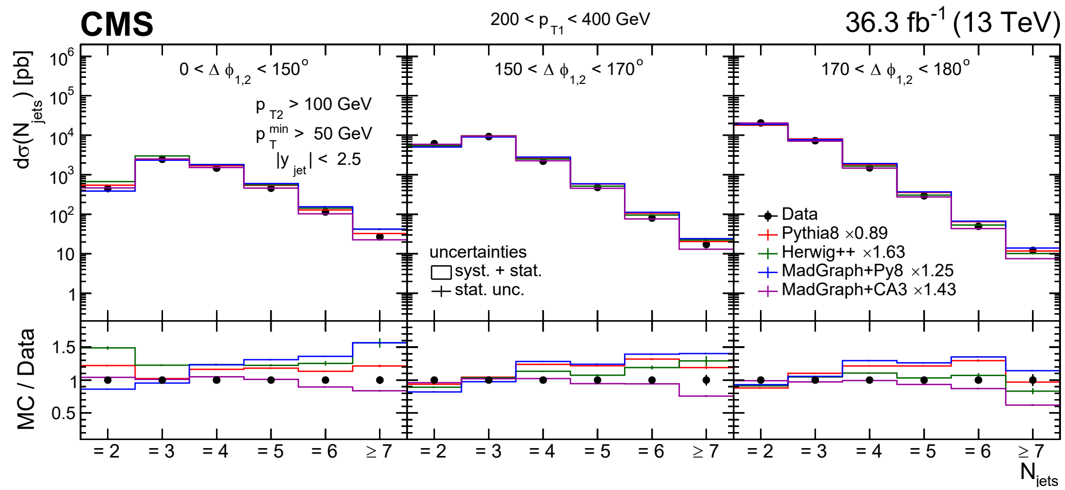

NLO dijets calculations with PB TMD PDF with TMD parton showering describe low-multiplicity region with less amount of tunable parameters then with conventional parton showering

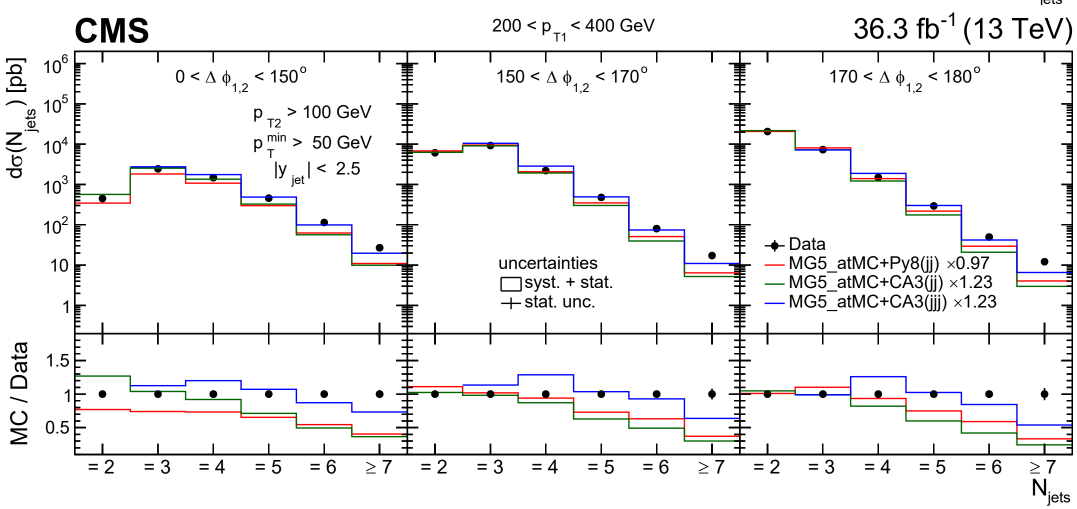

Noone generator describes Full jet mulyiplicity range and p_T dependence up to 4th jet

EPJC 83(2023)742
CMS PAS-SMP-21-006

W+c: strange quark PDF

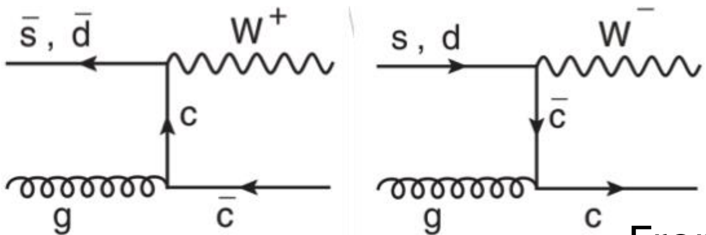

$$R_s = \frac{s + \bar{s}}{\bar{u} + \bar{d}}$$

From neutrino scattering Rs=0.5
At Q2=1.9 GeV2 strange sea-quark density is suppressed
ATLAS: W,Z - strange sea-quark density is enhanced – seen only by ATLAS

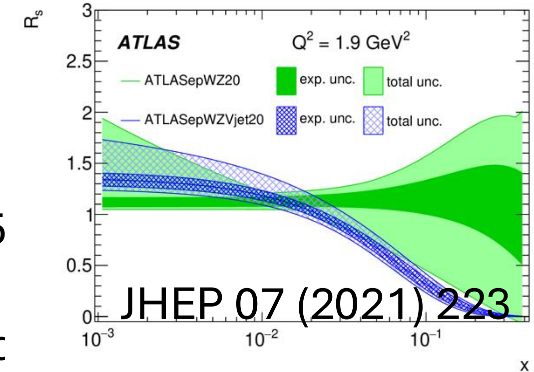

JHEP 07 (2021) 223

PDFs are probed at
$< x > \approx 0.007$
at the scale of W mass

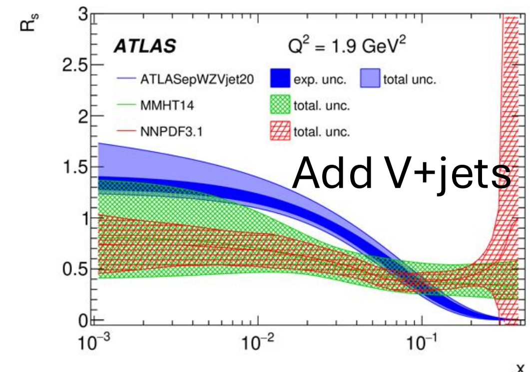

Add V+jets

13 TeV (CMS, 36 fb^{-1}):
σ (W + c) = 1026 ± 31 (stat) ± 72 (syst) pb

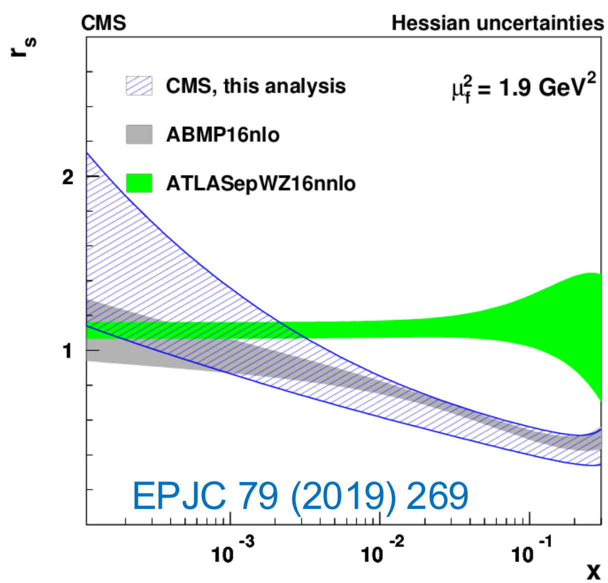

EPJC 79 (2019) 269

EPJC 84 (2024) 27

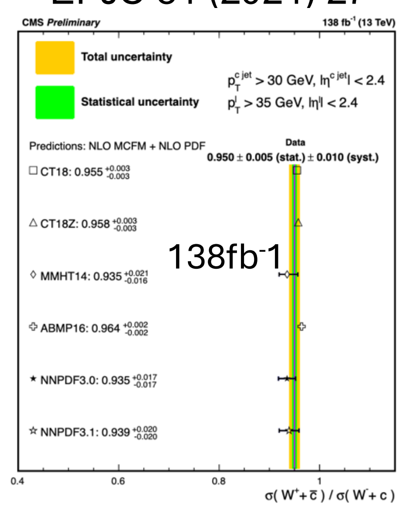

138fb-1

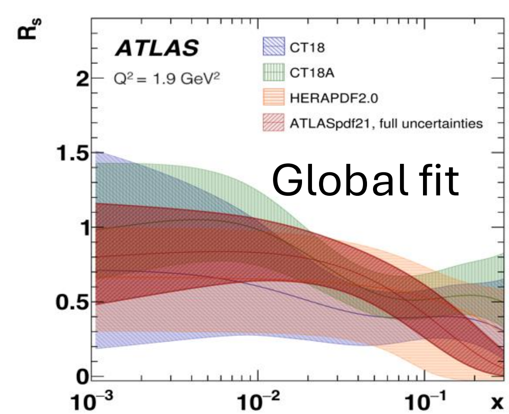

Global fit

EPJC 82(2022)438

Perturbative QCD (pQCD)

pQCD prediction at fixed order calculation
Singularities (soft and collinear) are:

- ❑ **partially cancelled between real and virtual contributions,**
- ❑ **partially absorbed in PDFs and coupling renormalizations**

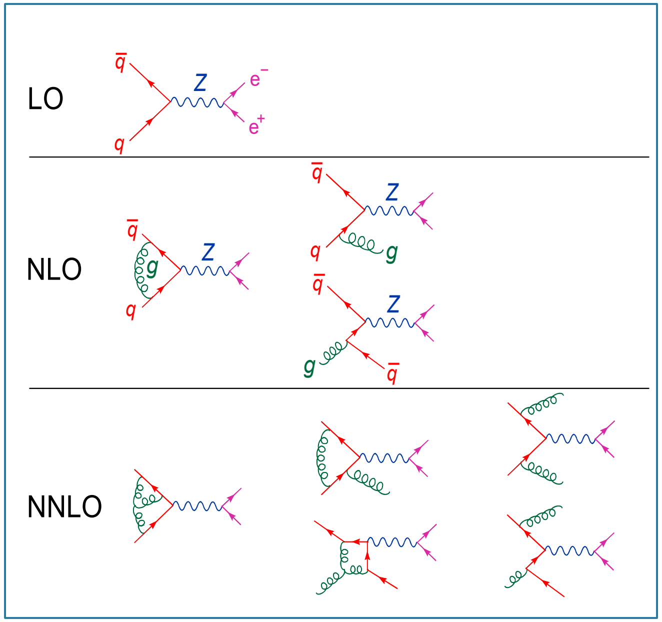

Finally, fixed order QCD calculations are matched with parton showers (PYTHIA or HERWIG) Monte-Carlo models which represent soft and collinear radiation patterns
OR in alternative approach non-perturbative and Electroweak corrections are applied as weights

NP corr — PS corr — EWK corr

pQCD X

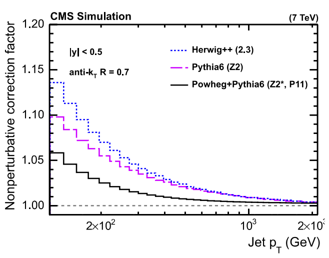

X

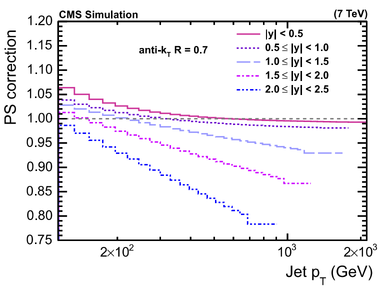

X

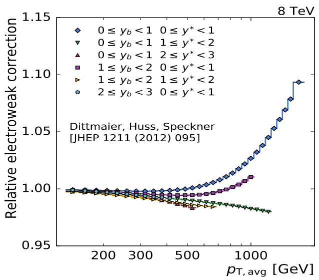

http://www.slac.stanford.edu/cgi-wrap/getdoc/slac-pub-13054.pdf

QCD Evolution equation

Connection between various scales in QCD (for instance, between PDF and the high-momentum scattering) is performed via evolution differential equations.

In small-x region standard approach to NLO QCD perturbative calculations. DGLAP (expansion in terms of power of $a_S \ln(Q^2)$) is predicted to be not sufficient.

Need to develop alternative approaches:

- BFKL (expansion in terms of $\ln(1/x)$).
- CCFM angular and energy ordering
- LDC (Linked dipole chain)
- …

Non perturbative effects, Multi Parton Interaction (MPI) etc. models have to be tuned to data.

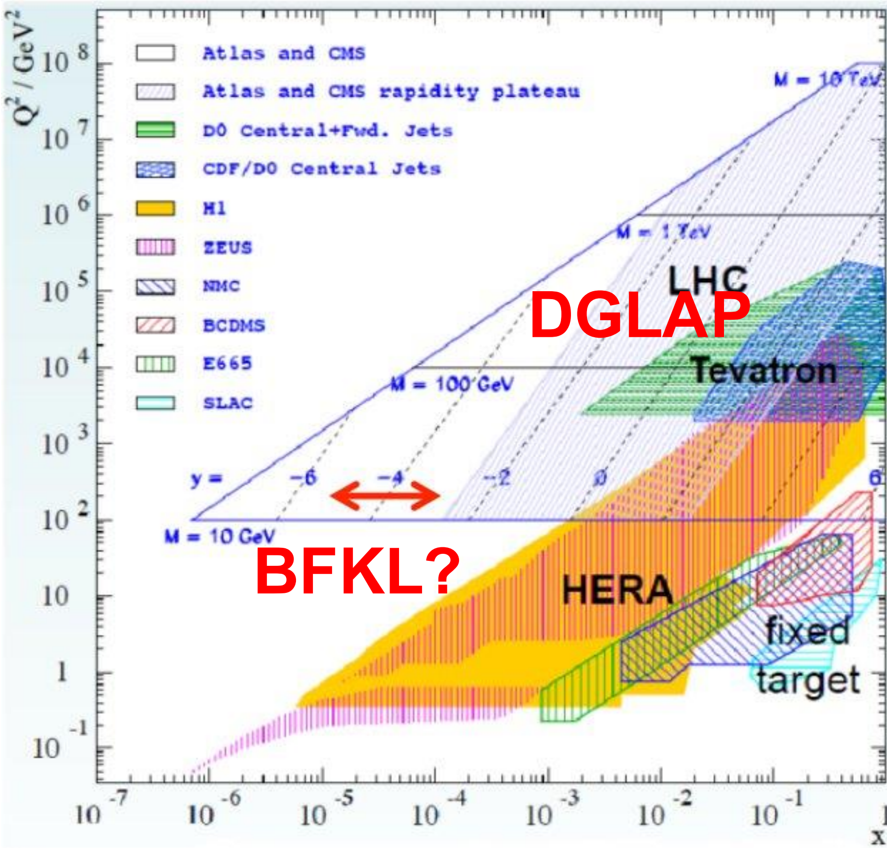

Jet clustering technique

Fixed cone algorithms:

Iterative Cone (CMS) / JetClu (ATLAS)
Midpoint algorithm (CDF/D0)
Seedless Infrared Safe Cone (SISCone)

Iterative cone

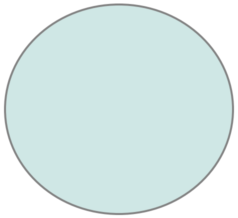

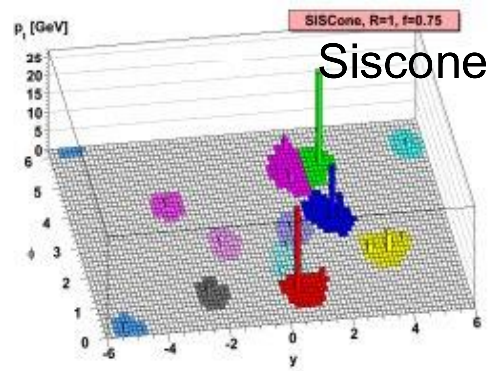

Successive recombination algorithms:

$$d_{ij} = min\left(k_{ti}^{2p}, k_{tj}^{2p}\right)\frac{\delta_{ij}^2}{R^2}$$

$$d_{iB} = k_{ti}^{2p}$$

if($d_{ij} < d_{iB}$) add i to j
and recalculate p_j

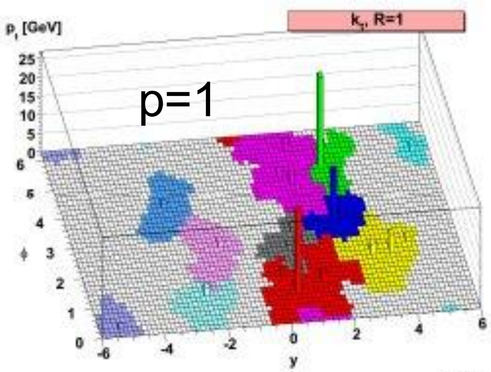

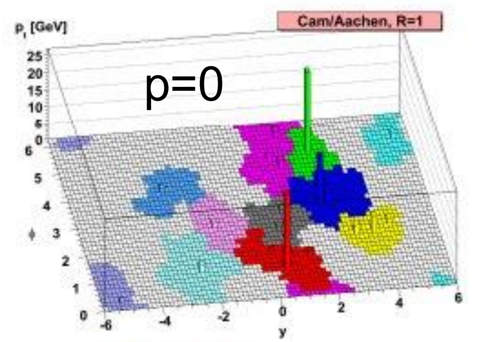

p=1 ->k_T jet algorithm
p=0 ->CA jet algorithm
p=-1 ->"Anti-k_T" jet algorithm

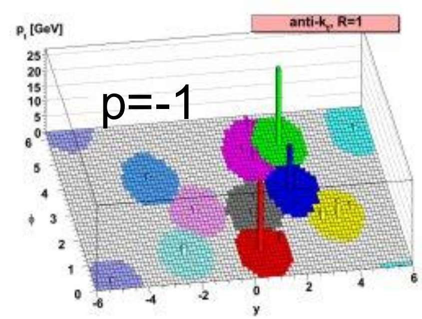

CMS uses R=0.5,0.7 in Run1
R=0.4,0.6 in Run2
ATLAS uses R=0.4,0.6 in Run1,2

JHEP 1009 (2010) 091

Jet reconstruction in detector

Calorimeter jets (CaloJets):
Jet clustered from Calorimeter Towers (CMS,ATLAS) Or TopoClusters (ATLAS)
CaloMET

Anti-Kt clustering algorithm is applied to the different objects

Tracker jets (TrackJets):
Jet clustered from Tracks

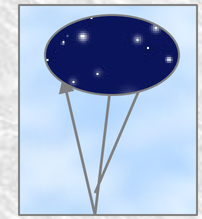

Subdetectors: Tracker

(ATLAS,CMS, ALICE)

ParticleFlow jets (PFJets):
Jet clustered from Particle Flow objects (a la generator level particles) which are reconstructed based on cluster separation.
Subdetectors: ECAL,HCAL, Tracker, Muon

PFMET **CMS**

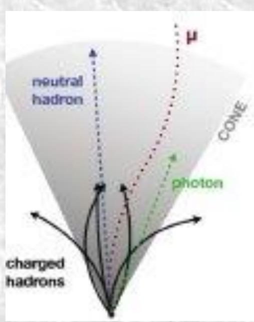

All subdetectors participate in reconstruction

The residual jet energy corrections is applied on top of all algorithms

JetPlusTrack jets (JPTJets):
Starting from calorimeter jets tracking information is added via subtracting average response and replacing with tracker measurements.
Subdetectors: ECAL,HCAL, Tracker, Muon
TcMET
CMS

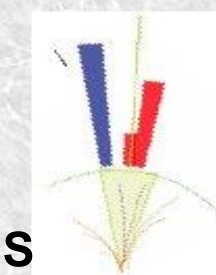

Addition to SMP-20-011
JHEP 02(2022) 142

Fixed pQCD at NLO and NNLO with NLOJet++ and NNLOJET
NLO calculation in FASTNLO.

$\mu_f = \mu_R = p_{Tjet}$ (or HT)

NLO improved to NLO+NLL using MEKS
PDF sets: CT14, NNPDF 3.1, MMHT2014 (includes 7 TeV ATLAS and CMS jet data), ABM16 (no 7 TeV jet data), HERAPDF 2.0 (HERA DIS only)

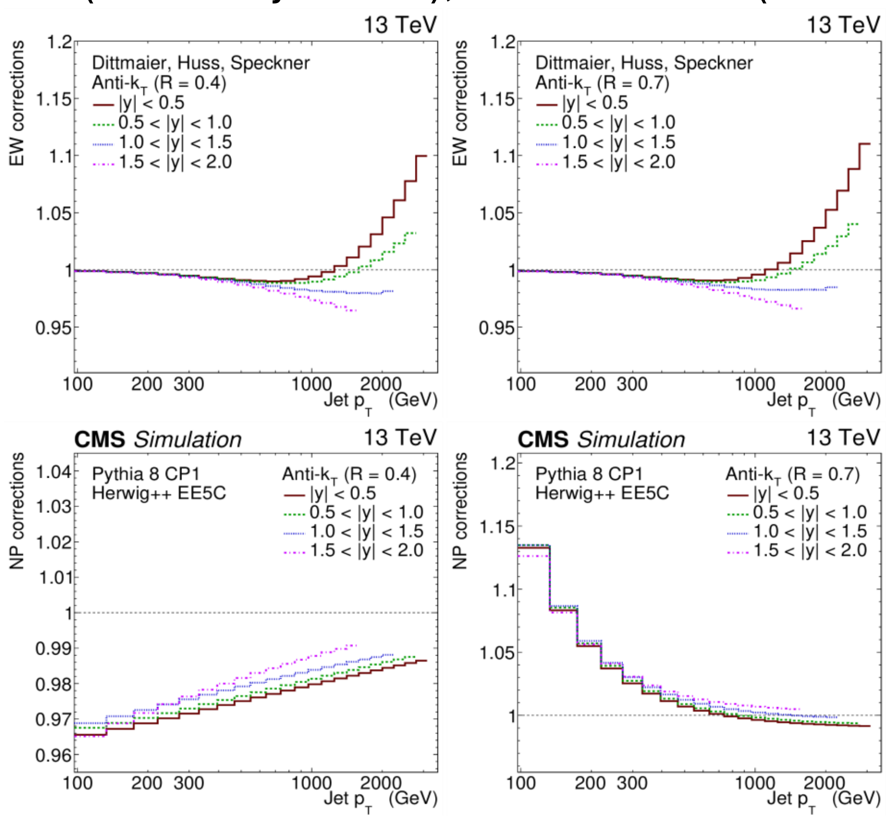

EWK Corrections
At NLO accuracy

NP corrections:
PYTHIA 8 CP1 tune
HERWIG++ EEC5 tune

Dead cone effect for heavy quarks

J. Physics G*: Nucl. Part. Phys.* **17** 1602: dead cone in soft gluon radiation by heavy qua

The dead cone size depends on m/E

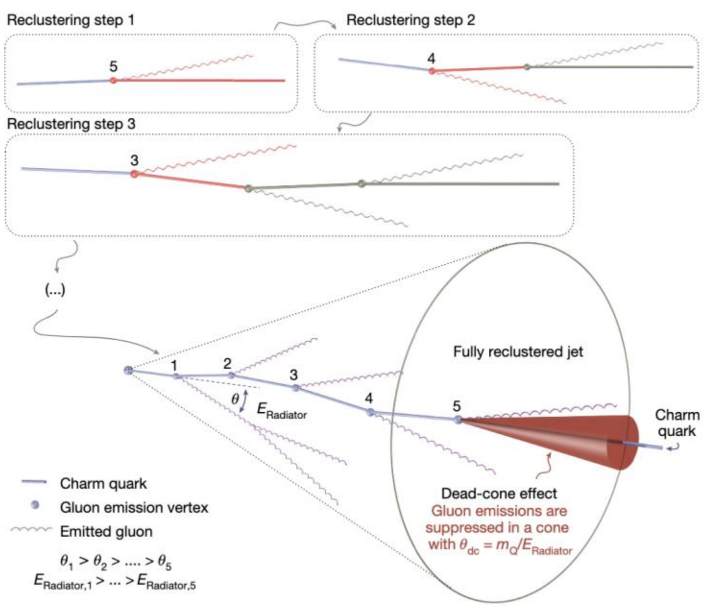

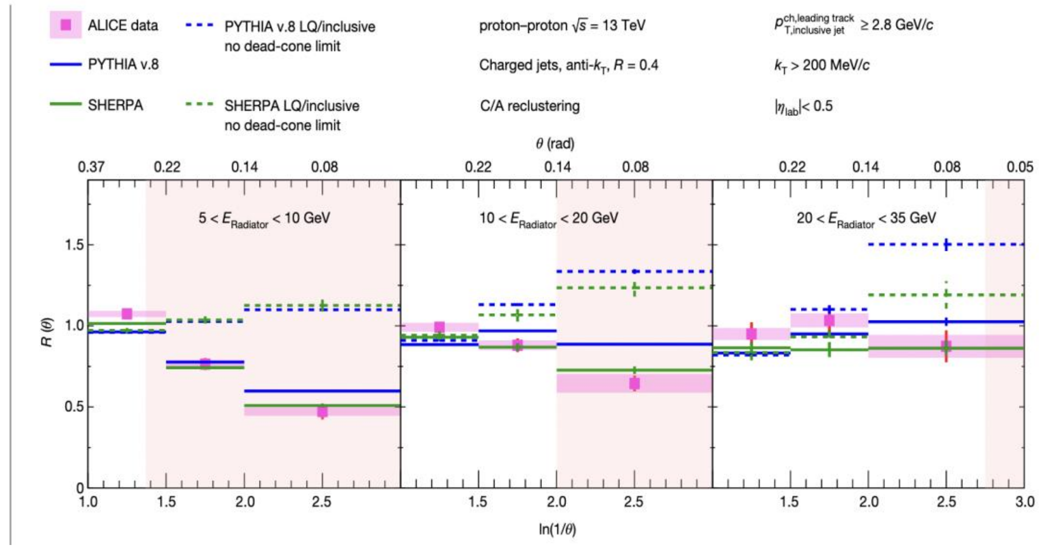

$$R(\theta) = \frac{1}{N^{D^0\text{ jets}}}\frac{dn^{D^0\text{ jets}}}{d\ln(1/\theta)} \Big/ \frac{1}{N^{\text{inclusive jets}}}\frac{dn^{\text{inclusive jets}}}{d\ln(1/\theta)}\Bigg|_{k_T, E_{\text{Radiator}}}$$

First direct observation of the dead cone effect.

ALICE: Nature volume 605, p. 440–446 (2022)

Azimuthal decorrelations

$\Delta\phi_{jj}$ in bins of p_{T1} for p_T>100 GeV, p_{T1}>200GeV, $|y_1|<2.5, |y_2|<2.5$

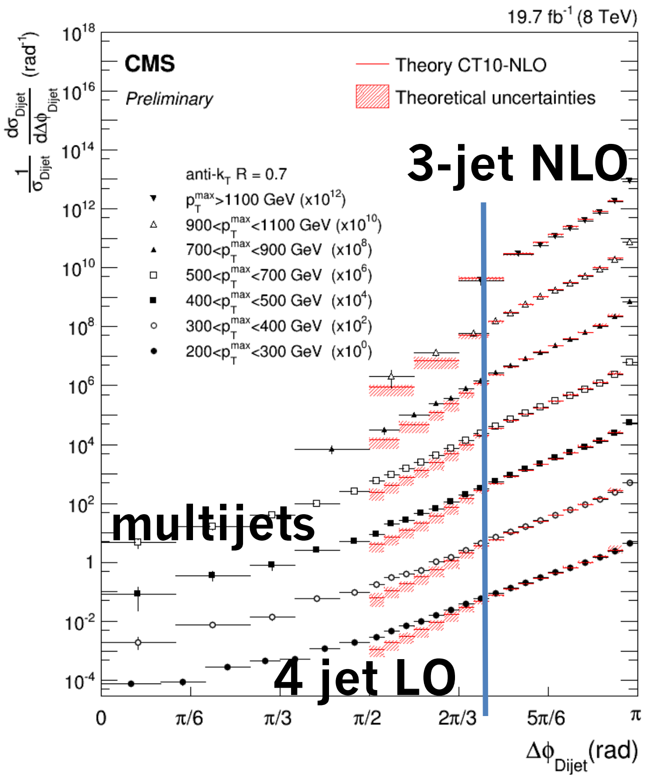

Comparison is done with fixed-order pQCD (NLO) and with LO ME+PS

Back-to-back region of dijet correlations-sensitive probe of soft gluon radiation

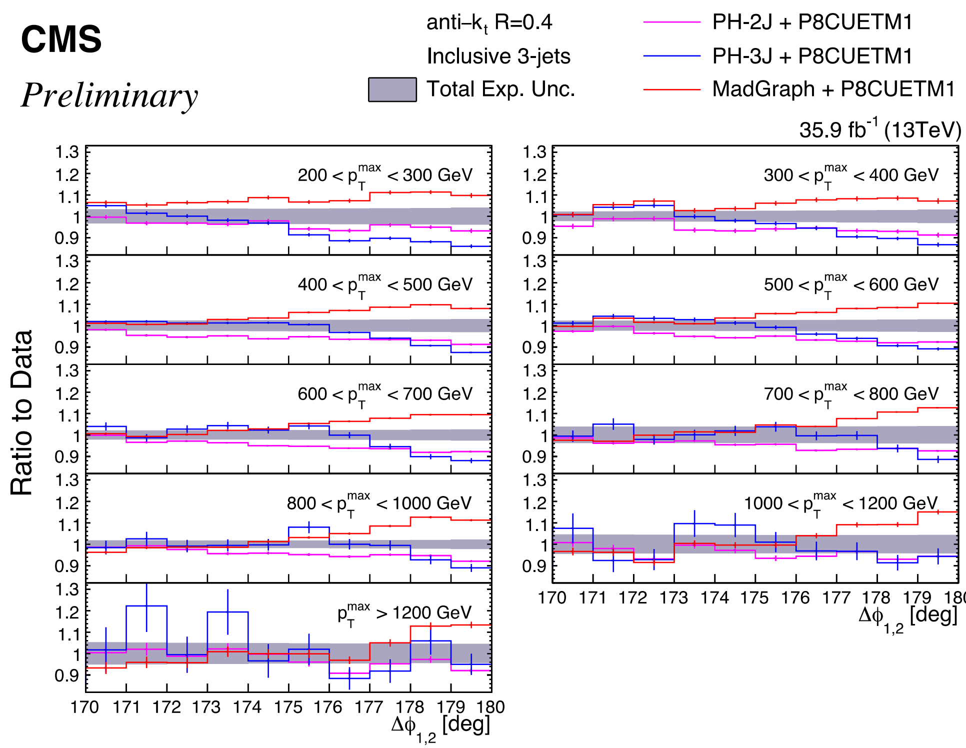

Deviations (~10%) are observed for all tested generators

EPJC 76 (2016) 536
CMS-PAS-SMP-17-009

Angular correlations of jets

- Events with at least two jets passing cuts: p_T>35 GeV in |η|<4.7
- For a pair of jets with the largest Δη (CMS) the angular distance is calculated: Δφ = φ1 – φ2

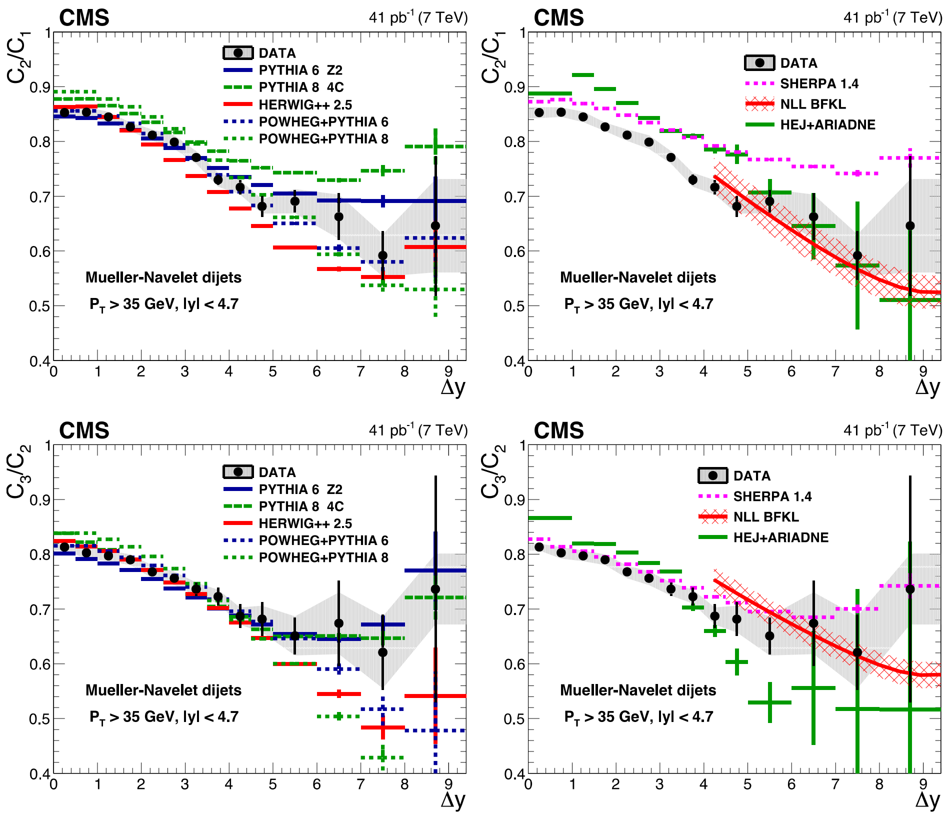

DGLAP generators start to be worse in high Δy description

Analytical BFKL calculations at NLL accuracy with an optimized renormalization schema provide reasonable description of data for the measured jet variables at Δy>4

$$C_n(\Delta y, p_{Tmin}) = \langle \cos(n(\pi - \Delta\phi)) \rangle$$

JHEP08(2016)139